

**USE OF CROSSLINKED HYDROGELS FOR THE CONTROL OF
MACROMOLECULAR CRYSTALLIZATION**

by

Andry Rafael Cera Manjarres

A thesis submitted in partial fulfillment of the requirements for the degree of

MASTER OF SCIENCE

in

CHEMICAL ENGINEERING

UNIVERSITY OF PUERTO RICO

MAYAGÜEZ CAMPUS

2012

Approved by:

Patricia Ortiz Bermudez, PhD
Member, Graduate Committee

Date

Juan Lopez Garriga, PhD
Member, Graduate Committee

Date

Madeline Torres-Lugo, PhD
President, Graduate Committe

Date

Wilma Santiago Gabrielini, Professor
Representative of Graduate Studies

Date

Aldo Acevedo Rullán, PhD
Chairperson of the Department

Date

Abstract

Crosslinked hydrogels in protein crystallization is an area of continuous growth. The counterdiffusion technique is a novel method for the crystallization of proteins, which entails the minimization of convection effects, resulting in high quality crystals. The three layer implementation of this technique in capillary tubes with different diameters has been accepted for the crystallization of proteins, by using a precipitating solution which diffuses through a protein chamber containing a gel matrix that controls the diffusion process. The diffusional process using such systems can be controlled but cannot be widely manipulated. The use of crosslinked hydrogels in the middle chamber can be used to control the diffusion of the precipitant and the number and size of crystals. This research focuses on the role of the crosslinked hydrogels, which control the nucleation process in the proposed protein crystallization. The effects of polymer concentration and hydrogel mesh size on protein crystal size were studied. Some key experimental details of the proposed method were: (i) to prepare pre-polymer solutions at different concentration using protein solution as the dissolvent. (ii) to employ membranes or plugs of different polymer concentrations using water as the dissolvent to control diffusion of the precipitating agent. The above solutions were exposed to a UV light source to induce polymerization. The supersaturation wave in the protein chamber was followed indirectly by recording the crystallization front advance and the crystal size and morphology along the protein chamber.

The polymer and proteins used in this study were Poly-ethyleneglycol, insulin, glucose isomerase and lysozyme. The results showed that when lysozyme protein was employed, the nucleation and crystal growth could be controlled by changing the polymer composition in the plug and the protein chamber respectively. In the case of insulin and glucose isomerase it was found that it is possible to obtain crystals of previously reported morphologies by using PEG hydrogel. Mesh sizes were also measured and they varied from 10-20 Å. This research led to the conclusion that the use of crosslinked hydrogels is a potential option for macromolecular crystallization, given that diffusion control can be readily manipulated and the polymer hydrogel does not affect protein crystal quality.

Resumen

El potencial de hidrogeles entrecruzados en la cristalización de proteínas es un área en continuo crecimiento. La técnica de contradifusión es un nuevo método para la cristalización de proteínas, el cual reduce los efectos convectivos generando cristales de alta calidad. El arreglo experimental de 3 capas de esta técnica en capilares con diferentes diámetros, ha sido aceptada para la cristalización de proteínas, utilizando una solución de agente precipitante la cual difunde a través de la cámara de proteína por una una matriz de gel que controla el proceso de difusión. El proceso de difusión empleando este tipo de sistemas puede ser controlado pero no puede ser manipulado fácilmente. El uso de geles entrecruzados en la zona media de la cámara puede ser empleado para controlar el proceso de difusión del agente precipitante; por tanto el número y tamaño de cristales.

El objetivo principal de esta investigación es el estudio del efecto de la concentración y tamaño de poro para controlar el tamaño final de los cristales. Para realizar esto: i) diferentes soluciones de polímero fueron preparadas usando la proteína como disolvente y ii) membranas (plugs) de diferentes porcentajes de polímero fueron empleados usando agua como disolvente para controlar el proceso de difusión del agente precipitante. Ambas soluciones fueron expuestas a radiación ultravioleta para inducir polimerización. El desarrollo de la onda de supersaturación en la cámara de proteína fue seguido indirectamente registrando el avance del frente de nucleación, el tamaño y morfología a lo largo de la cámara de proteína. El proceso de cristalización se llevo a cabo empleando hidrogeles

entrecruzados de Poli (etilenglicol) (PEG) y proteínas modelos como: lisozima, insulina y glucosa isomerasa. Los resultados indicaron que cuando fue empleado lisozima el proceso de nucleación y el crecimiento del cristal puede ser controlado por cambios en la composición en el plug y por la influencia del polímero en la cámara de proteína respectivamente. En el caso de insulina y glucosa isomerasa se demostró que es posible obtener cristales de estas proteínas con similar morfologías a las reportadas en la literatura con hidrogeles de PEG. También, el tamaño de poro de los diferentes plug fue medido y variaron de 10-20 Å. Esta investigación nos permite concluir que el uso de geles entrecruzados es una potencial opción para la cristalización de macromoléculas debido a que el control de la difusión puede ser fácilmente manipulado mientras que la calidad del cristal no se ve afectada.

To the memory of my dear grandmother, Flora

To GOD for give me the opportunity to reach this goal

To my family for its support unconditional

Copyright © by
Andry Rafael Cera Manjarres
2012

Acknowledgments

I would like express my gratitude to Madeline Torres-Lugo for giving me the opportunity to be part of her excellent research group. I am thankful for all her guidance and suggestions during the development of this research, which allowed me to give an explanation of the phenomena that we studied. I would also like to give special thanks to Professor Jose A. Gavira who helped me to understand and analyze the principles the crystallization of biomacromolecules.

My sincere acknowledgment to the University of Puerto Rico- Mayaguez for the opportunity to accomplishment graduate studies. This research was supported in part by the National Institute of Health and IDeA Networks of Biomedical Research Excellence (NIH-INBRE 2P20-RR016470-09)

I gratefully thank to undergraduate students Katia Ortiz-Lugo, Perla Valencia and Melanie Santos Marrero that worked for successfully of this project. I cannot forget my labmates Magada Latorre, Janet Mendez , Karem Court, Merlis Alvarez, Amalchi Castillo, Jose Jimenez, Derikson Rivera, Monica Perez, Rebecca Caban, Elmer Zapata and Orlando Soto with whom I had good experiences and learned something from everyone .

Thanks to my friends : Ana, Liliana, Yashira, Eduardo, Leonardo, Jhon, Roberto, Edwin, Jose Luis, Eduardo, Andrea, Eduardo. Also, I would like to thank Aracelis Rosado who was always attending to the administrative management of development of the project.

Contents

ABSTRACT	II
RESUMEN	IV
1 INTRODUCTION	1
2 THEORETICAL BACKGROUND	4
2.1 HYDROGELS	4
2.2 PRINCIPLES OF PROTEIN CRYSTALLIZATION	9
2.2.1 The concept of Supersaturation	10
2.2.2 Nucleation	12
2.3 CRYSTALLIZATION METHODS	14
2.3.1 Vapor-Diffusion	15
2.3.2 Batch Crystallization	17
2.3.2 Counterdiffusion	18
3 LITERATURE REVIEW	22
4 OBJETIVES	27
5 MATERIALS AND METHODS	29
5.1 MATERIALS	29
5.2.1 Preparation of precipitating agent	30
5.2.2 Preparation of protein solution	31
5.2.3 Determination of protein concentration in the pre-polymeric solution	32
5.2.4 Protein encapsulation in PEG hydrogels, for the determination of the concentration effect	32
5.2.5 Preparation of counterdiffusion experiments in three layer configuration	34
5.2.6 Preparation of capillary counterdiffusion experiments	36
5.2.7 Determination of nucleation front rate	38
5.2.8 Determination of molecular weight of monomers ($Mn0$)	39
5.2.9 Raman spectroscopy	39
5.2.10 Mesh size of PEG hydrogels	40
5.2.11 X-ray diffracton	45
6 RESULTS AND DISCUSSION	47
6.1 DETERMINATION OF THE MESH SIZE	47
6.2 EFFECT OF PEG CONCENTRATION ON THE NUCLEATION OF LYSOZYME CRYSTALS	50
6.3 EFFECT OF LYSOZYME PROTEIN CONCENTRATION ON THE PROCESS OF NUCLEATION	56
6.4 EFFECT OF THE PLUG COMPOSITION ON THE SUPERSATURATION WAVE	65
6.5 HARDWARE PROTOTYPE FOR THE CONTROL FOR THE CONTROL OF PRECIPITATING AGENT DIFFUSION USING AD HOC PEG-PLUGS	71
6.6 GENERALIZATION OF THE USE OF PEG HYDROGELS IN CRYSTALLIZATION	73
7 CONCLUSIONS	76
8 REFERENCES	78
APPENDICES	87

Table of Figures

Figure 1. Representation of the mesh size (ξ) and molecular weight between crosslinks (M_c) on an idealized hydrogel network.....	9
Figure 2. Solubility diagram for crystallization from solution showing the labile, metastable, and undersaturated regions. Adapted from reference[26].....	11
Figure 3. Variation the activation free energy as a function of r . Adapted from ref. [28]	14
Figure 4. Phase diagram is illustrated showing the vapor diffusion process of crystallization. Adapted from ref [27]......	17
Figure 5. Phase diagram showing the batch process. Adapted from ref. [27]......	18
Figure 6. Two layer (a) and three layer (b) configurations of the counterdiffusion technique.	20
Figure 7. Phase diagram showing how counterdiffusion crystallization works. Adapted from ref [7]......	20
Figure 8. The experimental setup of other 3L configurations, using a) counterdiffusion Gel Acupuncture Method in a GAME and b) the prefilled Granada Crystallization Box Domino (GCBD). The protein solution (orange) fills the capillary. The physical buffer (violet) is agarose gel and the precipitating agent (blue gray) promotes nucleation. Adapted from references [3, 36]......	21
Figure 9. Experimental set up in three Layer configuration	36
Figure 10. Experimental set up in Granada box crystallization.....	38
Figure 11. Typical elements to prepare the membranes for determination of the mesh size by equilibrium swelling theory: a) Teflon mold and b) experimental set up.....	41
Figure 12. Typical elements to prepare the samples of determination of the mesh size by Rubber Elasticity theory: a) Teflon mold and b) experimental set up.	45
Figure 13. Determination of mesh size of the different PEG plug compositions employed to control diffusion the precipitating agent obtained by equilibrium swelling theory (red bars) and rubber elasticity theory (green bars). Error bars represent standard error of the mean of the mesh size ($n= 4$ for rubber elasticity method and $n=8$ for equilibrium swelling). Statistical differences are considered when $p < 0.05$	49
Figure 14 Nucleation advanced front through the protein chamber of 5 % PEG hydrogel prepared with 40 mg/mL protein as a solvent.	53
Figure 15 Nucleation front rate of the precipitating agent through the protein chamber with different PEG compositions. Bars represent interval 95 % of confidence for hydrogels. Statistical differences are considered when $p < 0.05$	54
Figure 16. Pictures of lysozyme crystals grown at constant temperature in a PEG hydrogel and different polymer compositions in the prepolymeric solution of: (a) 5% , (b) 7% and (c) 9%, using a 40 mg/mL protein concentration, and (d)10% using a 70 mg/mL protein concentration. The scale bars represent 200 μm	55
Figure 17 Estructure agarose gel	57
Figure 18 Structure idealized of PEGMA/PEGDMA (1000) hydrogel. Monomer (---) and crosslinker (---).	58
Figure 19 Nucleation front advance vs. square root time. The hydrogels were prepared with a protein concentration of 40 mg/mL.....	61
Figure 20 Nucleation front advance vs. square root time. The hydrogels were prepared with a protein concentration of 50 mg/mL.....	62

Figure 21	Nucleation front advance vs. square root time. The hydrogels were prepared with a protein concentration of 60 mg/mL	63
Figure 22.	Pictures of lysozyme crystals grown at constant temperature in a 10% PEG hydrogel using protein concentration of: (a) 40 mg/mL (b) and 60 mg/mL. The scale bars represent 200 μm.	64
Figure 23	Pictures of lysozyme crystals grown at constant temperature in a 0.2 (w/v) agarose gel using protein concentration of: (a) 40 mg/mL (b) and 60 mg/mL. The scale bars represent 1000 μm.	64
Figure 24.	Pictures of lysozyme crystals grown at constant temperature in a 10% PEG hydrogel using PEG plug composition of 20% in different zones of the capillaries: (a) initial,(b) medium and (c) final. The scale bars represent 200 μm.	69
Figure 25.	Pictures of lysozyme crystals grown at constant temperature in a 0.2% (%w/v) agarose using different PEG plug composition: (a) 20 , (b) 35 and (c) 50% respectively. The scale bars represent 500 μm.	69
Figure 26.	Nucleation front rate of the precipitating agent through the protein chamber (10%) PEG hydrogel and agarose gel (0.2 % w/v) for each employed PEG plug and its respective mesh size obtained by equilibrium swelling. Bars represent interval 95 % of confidence for hydrogels. In the case of mesh size the bars represent the standard deviation. Statistical differences are considered when $p < 0.05$.	70
Figure 27	Device to crystallize macromolecules based on the principle of counterdiffusion using a three layer arrangement	72
Figure 28	Pictures of insulin crystals grown at constant temperature in a 10% PEG hydrogel using protein (20mg/mL) as a solvent. The scale bars represent 100 μm.	74
Figure 29	Pictures of glucose isomerase crystals grown at constant temperature in a 10% PEG hydrogel using protein solution (30mg/mL) as a solvent. The scale bars represent 200 μm.	75
Figure 30.	Pictures of glucose isomerase crystals grown at constant temperature in a 10% PEG hydrogel using protein solution (70mg/mL) as a solvent. The scale bars represent 100 μm	75

List of Tables

Table 1. Characteristics and examples of natural and synthetic gels	5
Table 2. Strategies for creating supersaturation. Adapted from reference [29]	15
Table 3. The Precipitating agent of proteins	31
Table 4. Experimental design	33
Table 5. Polymerization conditions of the different plug of PEGMA/PEGDMA	35
Table 6. Polymerization conditions of the different protein chambers of PEGMA/PEGDMA	37
Table 7. Polymerization conditions of the PEG hydrogels for equilibrium swelling characterization.	41
Table 8. Polymerization conditions of the membranes of PEGMA/PEGDMA at the same composition of the plug.....	43
Table 9 Ratio of the Grashof number among differents PEG plug compositions.....	68

List of Appendix

Appendix 1. Determination of molecular weight of monomers (Mn_0) by ($^1\text{H-NMR}$)	87
Appendix 2. Raman spectroscopy	93
Appendix 3. X-ray diffraction.....	95
Appendix 4 Nucleation advanced front trough the PEG hydrogel at different compositions.....	97
Appendix 5. Nucleation advanced front trough the 10 % PEG hydrogel at different protein concentrations.....	98
Appendix 6. Nucleation advanced front trough the 10 % PEG hydrogel at different PEG plug composition	100
Appendix 7. Nucleation advanced front trough the 0.2 % w/v agarose gel at different PEG plug composition	102

1 INTRODUCTION

Due to significant progress in molecular biology, there is a need for atomic level characterization of macromolecular structures for applications in human medicine, agriculture, and industrial processes [1]. There are a number of methods that produce structural and dynamic data, but for the purposes of atomic level structure determination, X-ray crystallography is the most adequate. Characterization by X-ray crystallography is absolutely dependent on the availability of crystals of the macromolecule of interest; the crystals must be of sufficient size and quality to permit accurate data collection. To obtain high quality crystals, it is necessary to reduce mass transport by convection during the crystallization process because it affects the absorption and incorporation of impurities in the crystals [2]. These impurities, in turn, affect the size, morphology development and perfection of the crystals. To solve this problem, crystal growth techniques have been developed that limit convective mass transport by employing hydrogels, micro-channels, capillaries and/or microgravity[3]. Crystals grown under these conditions have well-developed facets and possess excellent diffraction properties. Moreover, despite the fragility of the crystals caused by the high quantity of water in their structure (usually takes values in the range 70-80%) [4], they can be extracted from the hydrogels without damage. In the absence of the gel, similar crystal quality can only be obtained under reduced gravity [4].

Chemically crosslinked gels like silica and physically crosslinked gels such as agarose have been successfully employed to obtain crystals of different proteins with a wide range of

molecular weights, isoelectric points and precipitating agents. Agarose gels have been found to increase nucleation, while silica gels reduce nucleation of some proteins [5].

The use of chemically crosslinked hydrogels has been successful in biomedical applications, specifically in areas like drug delivery and regenerative medicine. Their success is due to their biocompatibility, flexible methods of synthesis, range of constituents, and desirable physical and chemical characteristics [6]. However, the potential of crosslinked hydrogels in the crystallization of proteins is an area that has not been widely exploited. These hydrogels can be easily manipulated through changes in crosslink density and molecular weights of the precursor polymers. Therefore, this type of hydrogel could be used to obtain large crystals (at least 0.5 mm³) that can be characterized by X-ray and neutron diffraction. Also, these hydrogels have the potential to be useful for crystallization of other types of macromolecules such as membrane proteins which have amphiphilic surfaces and tend to form aggregates instead of crystals.

Recently, the interest for studying macromolecule crystallization using the counterdiffusion technique has increased, because it produces high quality protein crystals [7]. This technique combines the benefits of mass transport and physiochemical effects of a gel on protein crystallization and can be used in different geometrical arrangements. A precipitating agent is used to promote the formation of protein crystals in a gel inside a capillary tube. The gel reduces convective transport during the process of crystallization and therefore, high quality crystals are obtained.

Moreover, the properties of crosslinked hydrogels can be easily tailored according to the application. We used poly (ethylene glycol) (PEG) hydrogels in the application of biological macromolecule crystallization, because they can be synthesized with control over crosslink density and molecular weight of the precursor polymers. Variation in synthesis variables results in PEG hydrogels with different mesh sizes which in turn have a direct effect on the rate of diffusion of the precipitating agent through the protein chamber. The effects of polymer concentration and hydrogel mesh size on the nucleation, crystal size and morphology, and crystal quality will be studied using the counterdiffusion technique. The mesh size of the PEG hydrogels will be varied by changing the polymer concentration and the resulting crystals will be analyzed to determine the effect. The results of this study will serve to choose the adequate PEG hydrogel conditions that guarantee to obtain the best crystals according to the requirements.

2 THEORETICAL BACKGROUND

The desire to produce high quality protein crystals for structure determination has led to interest in techniques that can produce them, such as the counterdiffusion technique [7]. This technique combines the use of gels and capillaries to promote diffusive transport during the process of crystallization. To understand how this technique works and the effect the gel has on the crystallization process, it is important to first understand how hydrogels are formed and their characteristics as well as how the crystallization process takes place.

2.1 Hydrogels

Hydrogels are three-dimensional networks formed from hydrophilic homopolymers or copolymers crosslinked to form polymer networks that swell in water [8]. In general, the crosslinked structure of hydrogels is a network of hydrophilic polymer chains whose junctions may be formed by strong chemical linkages, permanent or temporary physical entanglements, microcrystals, or weak interactions (such as hydrogen bonds). Hydrogels may exhibit drastic volume changes in response to specific external stimuli, such as the temperature, solvent quality, pH, or electric field [9].

Hydrogels are either neutral or ionic, depending on the ionization of pendant groups. The network structure may be amorphous or semi-crystalline. In addition, hydrogels can be classified according to their porous structure as macroporous (pores of $\sim 10\text{-}200\ \mu\text{m}$), microporous (pores of $\sim 1\text{-}10\ \mu\text{m}$), and non-porous (pores of $< 1\ \mu\text{m}$) [10]. They can also be

classified based on their composition as synthetic or natural. Some general characteristics of hydrogels are summarized in Table 1.

Table 1. Characteristics and examples of natural and synthetic gels

	Natural polymer	Synthetic polymers
Examples	-Polysaccharides like dextran, chitin and agarose. -Proteins like collagen and gelatin [11]	-Poly(acrylic acid), poly(acrylamide), poly(N,N-dimethylacrylamide), Poly(ethylene glycol) (PEG) [12]
Advantages	-Generally have high biocompatibility-Biodegradable [11] -Low toxicity by-products	-Designed molecular weight and crosslinking density -Mass produced -Can be tailored to give a wide range of properties according to requirements [13, 14] -Low immunogenicity -Minimal risk of biological pathogens
Disadvantages	-Purity and pathogen content from sources [15] -Low mechanical strength [16] -Lack of reproducibility [15]	-Low biodegradability -Include toxic substances

When a gel is submerged in a fluid, the degree of swelling is governed by equilibrium between elastic retractive forces of the polymer chains and the thermodynamic compatibility of the polymer and the solvent [17]. In terms of Gibbs free energy, the system can be described by:

$$\Delta G_{total} = \Delta G_{elastic} + \Delta G_{mixing} \quad Eq. (1)$$

where $\Delta G_{elastic}$ is the contribution due to the elastic forces and ΔG_{mixing} represents the thermodynamic compatibility of the polymer and the solvent [18].

Differentiation of this equation with respect to the number of moles of solvent, keeping constant temperature and pressure, results in an expression in terms of chemical potentials:

$$\mu_1 - \mu_{1,0} = \Delta\mu_{elastic} + \Delta\mu_{mixing} \quad Eq. (2)$$

where, μ_1 is the chemical potential of the solvent in the polymer gel and $\mu_{1,0}$ is the chemical potential of the solvent outside the gel. The elastic contribution, $\Delta\mu_{elastic}$, can be determined from elasticity theory, while the change in chemical potential due to mixing, $\Delta\mu_{mixing}$, can be expressed as a function of enthalpy and entropy mixing [9]. For a highly crosslinked hydrogel, the polymer segments between crosslinks are short and do not assume a Gaussian distribution. The elastic contribution for the chemical potential of this type of gel is [19]:

$$\Delta\mu_{elastic} = \frac{NRTV_1}{\bar{v}M_c} \ln \left[1 - \frac{3}{M_c} v_{2,s}^{-2/3} + 3 \left(\frac{M_r}{\lambda M_c} \right)^2 v_{2,s}^{-4/3} - 3 \left(\frac{M_r}{\lambda M_c} \right)^6 v_{2,s}^{-2} \right] \quad Eq. (3)$$

Meanwhile, the contribution due to mixing is [20]:

$$\Delta\mu_{mixing} = RT \left[\ln(1 - v_{2,s}) + v_{2,s} + \chi_1 v_{2,s}^2 \right] \quad Eq. (4)$$

In these expressions, R is the universal gas constant, T is the absolute temperature, \bar{v} is the specific volume of the polymer, V_1 is the molar volume of water, λ is the number of bonds the monomer forms during polymerization, which for vinyl monomers is two, $v_{2,s}$ is the volume fraction of the polymer in the swollen hydrogel, M_r is the molecular weight of the

initial monomer, χ_1 is the polymer–solvent interaction parameter, and \bar{M}_c is the average molecular weight of the polymer segments between crosslinks. The value of \bar{M}_c can be determined by two experimental methods: equilibrium swelling and mechanical testing [20].

At equilibrium, $\Delta\mu_{elastic} = -\Delta\mu_{mixing}$; substituting the corresponding expressions, we obtain an expression for \bar{M}_c in terms of experimentally measurable variables [19]:

$$\frac{1}{\bar{M}_c} = \frac{2}{\bar{M}_n} - \frac{(\bar{v}/V_1)[\ln(1 - v_{2,s}) + v_{2,s} + \chi_1 v_{2,s}] \left[1 + \left(\frac{M_r}{\lambda \bar{M}_c}\right) (v_{2,s}^{1/3})\right]^3}{\left[(v_{2,s})^{1/3} - \frac{1}{2} v_{2,s}\right] \left[1 - \left(\frac{M_r}{\lambda \bar{M}_c}\right) (v_{2,s})^{1/3}\right]^2} \text{Eq. (5)}$$

If, however, the polymer is crosslinked in solution, one must adjust the elastic contribution resulting in the following expression [19]:

$$\frac{1}{\bar{M}_c} = \frac{2}{\bar{M}_n} - \frac{(\bar{v}/V_1)[\ln(1 - v_{2,s}) + v_{2,s} + \chi_1 v_{2,s}] \left[1 + \left(\frac{M_r}{\lambda \bar{M}_c}\right) (v_{2,s}^{1/3})\right]^3}{v_{2,r} \left[(v_{2,s})^{1/3} - \frac{v_{2,s}}{2v_{2,r}}\right] \left[1 - \left(\frac{M_r}{\lambda \bar{M}_c}\right) \left(\frac{v_{2,s}}{v_{2,r}}\right)^{1/3}\right]^2} \text{Eq. (6)}$$

Where $v_{2,r}$ is the polymer volume fraction in the relaxed state (i.e. immediately after crosslinking but before swelling).

An alternative way to measure \bar{M}_c is based on the resemblance that a hydrogel has to a rubber. In particular, both show elastic behavior when exposed to stress. Elasticity theory of polymers relates the elongation generated by the stress to \bar{M}_c [21-23]:

$$\bar{M}_c = \left[\frac{\left(\frac{\tau}{\alpha - 1/\alpha^2} \right)}{RTv_{2,s}(\rho 10^6)} + \frac{2}{\bar{M}_r} \right]^{-1} \quad Eq. (7)$$

Where τ , is the stress applied to the polymer sample, ρ is the density of the polymer, $\bar{M}_{n(0)}$ is the molecular weight of the monomer and α is the deformation ratio (deformed length / initial length). To obtain the required parameters, it is necessary to do the experiments using a tensile test system.

In addition to swelling, hydrogels can be used to restrict the transport of solutes. The maximum size of solutes that can diffuse through the gel is determined by the mesh size or correlation length (ξ) of the hydrogel (figure 1). In our case, the determination of this parameter is very important because the rate of transport of the precipitating agent through the hydrogel will have an effect on the nucleation rate. Also, the mesh size will restrict the growth of the protein crystals, which affects their form and size.

As was remarked above, both equilibrium swelling theory and rubber elasticity theory are useful to determine average molecular weight between crosslinks, \bar{M}_c . This molecular weight is related to the mesh size by [24]

$$\xi = l v_{2,s}^{-1/3} \left(\frac{2C_n \bar{M}_c}{M_0} \right)^{1/2} \quad Eq. (8)$$

In this expression, l is the length of the bond along the backbone chain, $v_{2,s}$ is the volume fraction of the polymer in the swollen hydrogel, C_n is the Flory characteristic ratio of the polymer, and M_0 is the molecular weight of the monomeric repeating units.

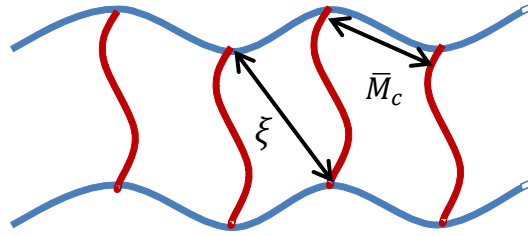


Figure 1. Representation of the mesh size (ξ) and molecular weight between crosslinks (\bar{M}_c) on an idealized hydrogel network.

2.2 Principles of protein crystallization

The preparation of large single protein crystals is a challenge being widely pursued. High quality protein crystals are necessary for the study of their structure by X-ray diffraction. The information about protein structure is fundamental for our understanding of protein function and for developments in biochemistry, pharmaceuticals, and biology.

Given the importance of protein crystal preparation, an understanding of the nucleation and growth of these crystals is necessary. These processes could be explained using the classical theory of crystallization of small molecules, which is perfectly valid for macromolecules[25]. However, there are two important differences between crystallization of small molecules and macromolecules: The first one is that proteins usually require a very high level of supersaturation for nucleation to take place, in comparison with small molecules[26]. The other is that when supersaturation is achieved there is competition between the formation of

crystals and amorphous precipitates. There are some other differences that make protein crystallization challenging. For example, proteins need a complex environment to avoid denaturalization; as a result, changes in the environment (e.g. pH) may induce changes in conformations that could inhibit the crystallization process. Also, the size of the macromolecules complicates their arrangement in a crystalline form[26]. All of these factors make protein crystallization a difficult and unpredictable endeavor.

One of the key aspects in the area of crystallization is to generate conditions that enhance protein solution supersaturation. Supersaturation will drive the protein to aggregate and start the process of nucleation [27].

2.2.1 The concept of Supersaturation

The solubility of macromolecules is a defined quantity that depends on physicochemical properties such as temperature, pH and ionic strength [28]. In a saturated protein solution, both solid and solution states coexist in equilibrium. Crystals cannot grow in this type of solution since equilibrium would drive the protein back into solution. To grow crystals, it is necessary to generate a supersaturated environment in which the aggregation of protein molecules is thermodynamically favorable, since the chemical potential of the protein in solution (μ) will be higher than that of the protein in crystal form (μ_c)[29]. As protein crystals grow, the concentration of protein in solution will decrease until the saturation condition is again reached ($\mu = \mu_c$). Once the equilibrium state is reached, the protein crystals will stop growing and can be isolated for their characterization.

One way to produce the supersaturated solution is to reduce the solubility of the protein in the solution by introducing a precipitating agent. The precipitating agent effectively moves the equilibrium condition to lower protein concentration. Figure 2 shows a solubility diagram in which the protein saturation concentration (blue line) is shown as a function of the concentration of precipitating agent. Thus, a protein solution that is undersaturated (below the blue line) can be made supersaturated (above the blue line) by introducing an adequate amount of precipitating agent, which would be equivalent to moving horizontally to the right on the solubility diagram [30].

To prepare high quality crystals, it is desirable to grow crystals near the equilibrium condition, since low saturation results in a slow and ordered development of crystals. In the solubility diagram, this region just above the saturation line is known as the metastable zone [28].

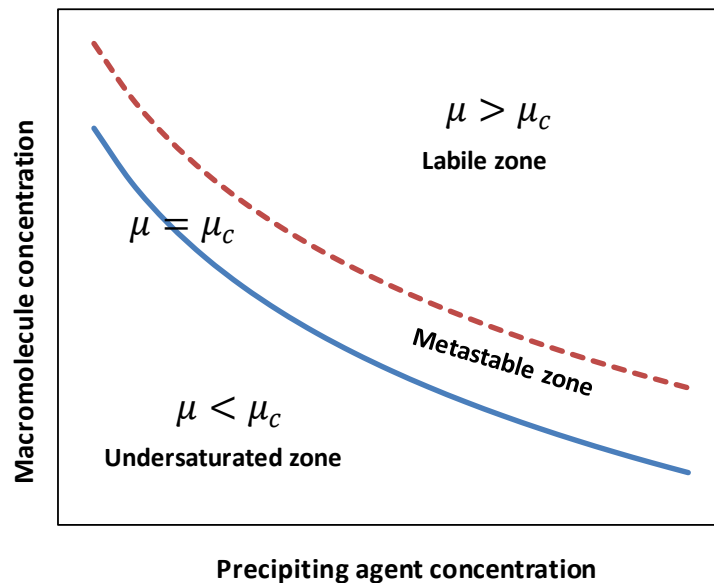


Figure 2. Solubility diagram for crystallization from solution showing the labile, metastable, and undersaturated regions. Adapted from reference [26]

2.2.2 Nucleation

In a supersaturated solution, some of the solute will form aggregates that eventually reach a critical size at which they become stable, a process called nucleation. Nucleation represents a first order phase transition in which the molecules pass from a wholly disordered state to an ordered one [28]. Nucleation may occur at surfaces in contact with the solution or on particles or bubbles suspended in the solution, a process called heterogeneous nucleation. Nucleation may also occur in the absence of nucleation sites within a uniform substance, a process known as homogeneous nucleation [31]. Even though nucleation is thermodynamically favorable in a supersaturated solution, there is an energetic barrier that must be surpassed due to the creation of a new interface. This barrier is smaller in the case of heterogeneous nucleation [28].

The change in free energy ΔG_r , associated with the formation of an aggregate of volumen V and surface S is [32]:

$$\Delta G_r = S\sigma - \frac{V}{v}kT\ln\beta \text{ Eq. (9)}$$

where σ represents the free energy associated with the surface between the aggregate and the solution, v is molar volume, T is the temperature, k is the Boltzman constant, and β is the supersaturation of the system (defined as the ratio between the actual concentration and equilibrium concentration, assuming identical activity coefficients in both cases). For an aggregate with spherical geometry with radius r , the equation can be rewritten as [33]:

$$\Delta G_r = 4\pi r^2 \sigma - \frac{4\pi r^3}{3\nu} kT \ln \beta \quad \text{Eq. (10)}$$

As an assumption, the surface tension of the small aggregates is considered to be the same as that of the macroscopic crystals. As Figure 3 illustrates, the values of ΔG^* increase with the size of the aggregate until it reaches the critical radius, r^* . Once the aggregates exceed this value, they are stable and crystal growth takes place [34].

It is possible to determine r^* by differentiation of equation (10) with respect to r resulting in the following expression [32]:

$$r^* = \frac{2\nu\sigma}{kT \ln \beta} \quad \text{Eq. (11)}$$

The maximum of the energy barrier ΔG^* is obtained by substituting r^* into equation 10 [32] :

$$\Delta G^* = \frac{16\pi\nu^2\sigma^3}{3(kT \ln \beta)^2} kT \ln \beta \quad \text{Eq. (12)}$$

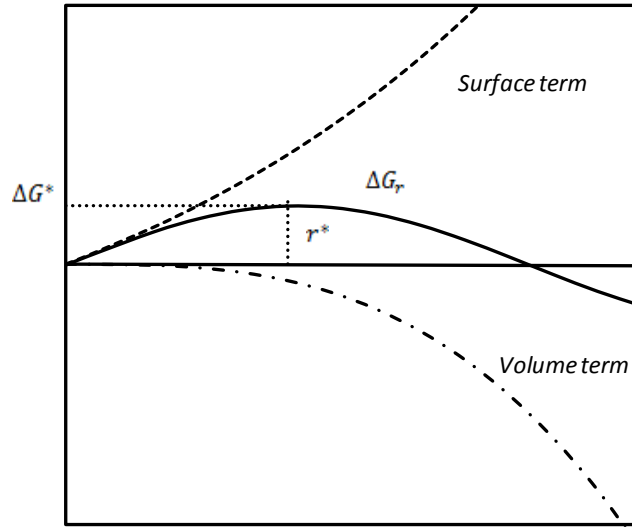


Figure 3. Variation the activation free energy as a function of r. Adapted from ref. [28]

The rate of nucleation (J) is defined as [28]:

$$J = A \exp\left(-\frac{\Delta G_r}{kT}\right) \text{ Eq. (11)}$$

In this expression, ΔG_r is analogous to the activation energy in a chemical reaction, but it is not constant since it is sensitive to changes in the level of supersaturation of the system. The pre-exponential factor A is a kinetic parameter that depends directly on the saturation level.

2.3 Crystallization Methods

There are different experimental methods that can be followed to obtain supersaturated protein solutions, which are required to grow protein crystals. Supersaturation can be the result of changes in the physical and chemical properties of the solution (See table 2).

Table 2. Strategies for creating supersaturation. Adapted from reference [29]

1. Direct mixing to immediately create a supersaturated condition (batch method)
2. Change in temperature
3. Addition of a precipitating agent
4. Change in pH
5. Addition of a ligand that changes the solubility of the solute
6. Alteration of the dielectric constant of the medium
7. Direct removal of water (evaporation)
8. Addition of polymer that produces volume exclusion
9. Addition of a cross-bridging agent
10. Removal of the solubilizing agent

For macromolecule crystallization, supersaturation is generally attained by the addition of a precipitating agent to the protein solution. There are two types of precipitating agents: salt and polymer. Both of them promote the precipitation of protein by reducing the water solvation layer that surrounds protein molecules, thus promoting protein aggregation[30].

The most common methods for macromolecule crystallization are vapor-diffusion and batch crystallization [26], but a novel technique known as counterdiffusion, which was initially applied to the crystallization of small molecules, is gaining relevance due to its ability to produce high quality crystals.

2.3.1 Vapor-Diffusion

The vapor-diffusion method consists of placing a drop of a solution of the protein and the precipitating agent (usually in a 1:1 ratio) in a chamber that contains a precipitating agent

solution with a concentration two times greater than that of the drop. The chamber is hermetically sealed and the system is allowed to reach equilibrium [28]. The water and volatile components in the drop migrate first to the vapor phase and then to the precipitating agent solution due to the concentration difference. As a result, the concentration of protein increases in the drop and reaches a supersaturation state. When the degree of supersaturation is high enough, nucleation takes place and the crystallization process continues.

This method presents several advantages; among them is that the system goes through several crystallization conditions as shown in the solubility diagram (See figure 4). Another advantage is the small amount of protein required, which in some cases is in the order of μL [35]; this is a critical advantage since the proteins used can be very expensive or of limited availability.

The vapor-diffusion method, however, also has some disadvantages. One of them is that mechanical perturbations, such as vibrations, can affect the shape of the drop and disturb the crystal growth. Also, when organic or volatile solvents are employed, changes in the drop shape can be induced by temperature fluctuations that can affect the liquid–vapor equilibrium. Another disadvantage is the difficulty in manipulating and transporting the sample for characterization [26].

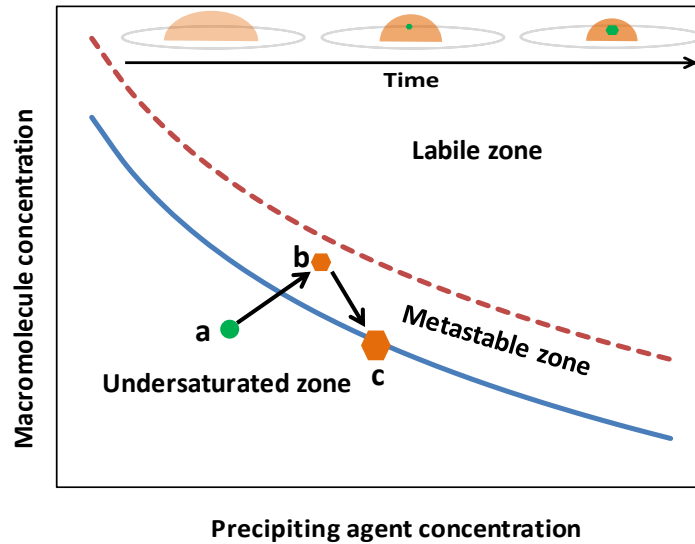


Figure 4. Phase diagram is illustrated showing the vapor diffusion process of crystallization. Adapted from ref [27].

2.3.2 Batch Crystallization

In this method a protein solution is directly mixed with a precipitating agent to form a supersaturated solution. If the conditions are appropriate, then nucleation will start immediately, followed by crystal growth. In contrast with the other methods, in the batch method, crystals start forming from a single condition, concentration, as shown in the solubility diagram of Figure 5. For this reason, the protein and precipitating agent concentrations must be carefully chosen [27]. In the case of unknown samples, however, multiple experiments are necessary to determine the optimal concentrations. With this technique there is a lack over control of the time spent in supersaturation conditions as it is determined by the rate of crystal growth [36]. This is obviously a difficulty for the majority

of macromolecules which generally require high supersaturation conditions to promote nucleation [26].

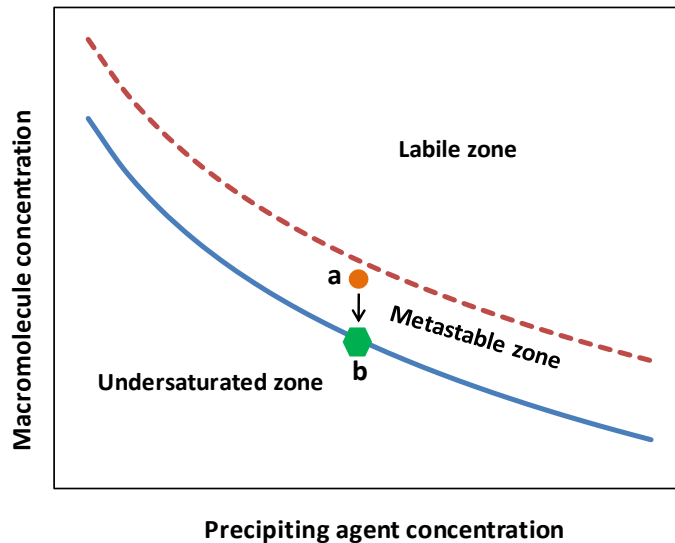


Figure 5. Phase diagram showing the batch process. Adapted from ref. [27].

2.3.2 Counterdiffusion

During the crystallization process, the transport of proteins in the solution affects the quality of the crystals. To obtain high quality crystals, mass transport in the system must be diffusion controlled. This can be achieved using gels, capillaries or microgravity [7]. Gels were first employed in the crystallization of macromolecules at the end of the last century [5]. They have been widely used because their presence reduces convection around the crystal faces during growth. Hydrophilic gels such as agar, silica and polyacrylamide have been tested for this purpose [37].

Counterdiffusion in capillaries is a simple, cost-effective and practical procedure to screen a wide range of supersaturation conditions in a single experiment. In the counterdiffusion technique, two solutions are needed: one of the protein solution and the other of the precipitating agent. The solutions are put in contact to promote diffusion into each other [27]. The solutions can be placed in direct contact or separated by a physical barrier also known as a plug. The first arrangement is known as a two layer (2L) arrangement and the latter as a three layer (3L) configuration (see Figure 6).

Once the solutions are put in contact, the precipitating agent diffuses gradually into the protein chamber, increasing the supersaturation and therefore precipitating the protein. As illustrated in the solubility diagram (Figure 7), the concentration of the precipitating agent is the near the interface, the highest promoting the maximum state of supersaturation in the system; at this point a large number of small crystals are formed. As time and the distance from the interface increases, the degree of supersaturation decreases and the rate at which supersaturation increases also decreases resulting in more time for crystal growth and therefore producing larger crystals.

Devices developed to carry out counterdiffusion experiments include the Granada Crystallization Box (GCB), the Granada Crystallization Box Domino (GCBD) and the Gel Acupuncture Method (GAME). All have the same principle of operation and the differences between them relate to the control of the level of supersaturation and consequently the nucleation and crystal growth (See figure 8).

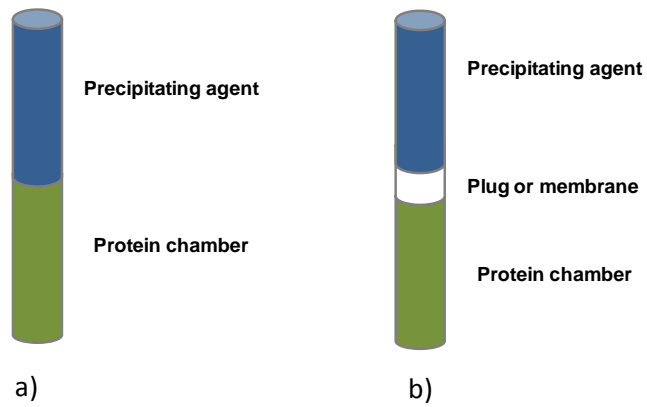


Figure 6. Two layer (a) and three layer (b) configurations of the counterdiffusion technique.

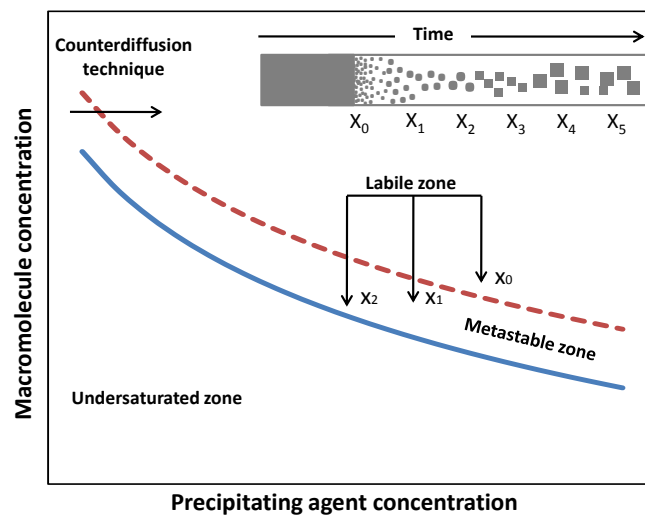


Figure 7. Phase diagram showing how counterdiffusion crystallization works. Adapted from ref [7].

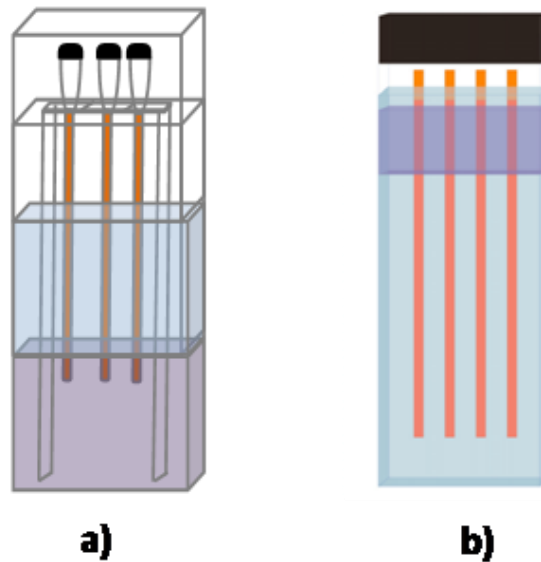


Figure 8. The experimental setup of other 3L configurations, using a) counterdiffusion Gel Acupuncture Method in a GAME and b) the prefilled Granada Crystallization Box Domino (GCBD). The protein solution (orange) fills the capillary. The physical buffer (violet) is agarose gel and the precipitating agent (blue gray) promotes nucleation. Adapted from references [3, 36].

3 LITERATURE REVIEW

The use of gels in the crystallization of macromolecules by counterdiffusion has proved more effective than conventional methods such as vapor-diffusion and batch crystallization because the elimination of convective flow, sedimentation, and buoyancy effects results in high quality crystals [38]. Several counterdiffusion experimental setups that combine gels and capillaries have been reported.[3, 36] Reports that demonstrate the advantages of protein crystallization using counterdiffusion with gels are discussed below.

Before their use for crystallization of proteins, gels had already demonstrated effectiveness in the crystallization of inorganic molecules [5]. More important was the observation that reduction of convective transport improved the quality of crystals [39]. It was not until 1988, when Robert et al. performed a systematic study were the potential of this technique for protein crystallization was demonstrated [5]. It has been reported that other protein crystallization techniques (e.g. vapor-diffusion and batch) present difficulties for the transfer of crystals to X-ray capillaries due to their mechanical instability [40]. However, the most critical issue is the manner in which supersaturation is achieved. For example, in batch crystallization, several experiments are needed to find optimal concentrations [41, 42]. This problem is avoided by the counterdiffusion technique since nucleation and growth of crystals proceed by changes in the level of supersaturation along the length of the system in which diffusive mass transport dominates [42]. Two effective ways to limit convective mass transport are the use of capillaries and gels. Based on this information, Garcia-Ruiz et al.

suggested the application of gels in different counterdiffusion configurations for protein crystallization [43].

In 1993 Garcia-Ruiz, presented a simple method known as Gel Acupuncture Method (GAME) which consisted of the combination of gels and capillaries [41]. In this method a gel is punctured with a capillary filled with protein solution or protein in a gelled medium. After puncture, the precipitating agent is added and diffuses through the gel until it reaches the capillary where crystallization takes place. The advantages of this method are that it permits X-ray diffraction of the crystals inside the growth environment and it reduces the amount of protein required because of the small diameter of the capillaries employed. The high quality of the crystals produced by this technique was demonstrated by Garcia-Ruiz et al. growing lysozyme crystals which were characterized by X-ray diffraction [44]. This was followed by research that employed several gels, capillaries of diverse diameters and forms, as well as various proteins and precipitating agents [41]. Of note is that the gels that gave the best results were silica gel and agarose, and the precipitating agents tested were comparable with those used regularly in other techniques such as vapor-diffusion. In all cases, single crystals were obtained, which took the form of the capillary, with the size and quality required for X-ray diffraction [41]. This method has been widely used for crystallization of a great variety of proteins, using different gels and capillary diameters [41, 45].

Garcia Ruiz et al. further developed the technique with a new device that works under the same principle as GAME, but has a major advantage ease of preparing counterdiffusion experiments. This device takes up less space and allows safe transport of the samples, e.g. for

X-ray diffraction analysis. Additionally, this device makes it possible to follow the crystallization process by microscopy as a result of the transparency of the capillary [36]. These advantages make this device ideal for the systematic study of crystallization of macromolecules of different molecular weights and isoelectric points, as well as different precipitating agents and gels [36, 46, 47].

The most widely used gels for macromolecular crystallization are silica gel and agarose. Silica gel has been widely employed for crystallization of proteins, viruses and nucleic acids [42, 44, 46, 48]. This chemical gel presents stability in a wide range of pH, precipitating agents, and buffers. Also, this gel is easy to prepare and of low cost [43]. However, it has been found that at $\text{pH} > 7$ it produces byproducts that can affect the properties of the macromolecules [4].

Agarose is a physical gel that is commonly used in biological laboratories for electrophoresis and as a culture medium. This gel is stable in a pH range between 3 and 9 and presents good mechanical properties at low concentrations [49]. However, the pore sizes of the gel change according to the nature and concentration of additives. Agarose has been used to prepare crystals of complex RNA-binding proteins among others [47].

The effect of the gel on the nucleation process has been studied by different techniques such as dynamic light scattering (DLS), small angle X-ray scattering (SAXS), and small angle neutron scattering (SANS) [50]. For example, SANS was used to observe that silica gel has an inhibiting effect on nucleation, which was explained by the adsorption of protein molecules on the gel surface due to hydrogen bonding interactions followed by a decrease in

the concentration of free protein in the medium [51]. In contrast, agarose was found to promote nucleation. Aggregates form around the gel, thus initiating the nucleation process[52]. It has also been reported that agarose gel serves as a filter of impurities during growth of the crystals [52, 53].

The quality of the crystals obtained using these gels was characterized employing X-ray topography. Both gels were found to promote the formation of crystals of better quality than those grown in solution. However, the crystals grown in silica gels were of higher quality since misorientations present in the crystals were weaker than those present in crystals grown in agarose.[54]. The authors believe that the reason for this is that the protein that is adsorbed on the silica gel filters the free protein from other impurities in solution, thus resulting in higher quality crystals. Also, in the case of agarose, fibers from the gels were found inside the crystal; this did not, however, significantly affect the quality of crystals [49].

There are few reports of macromolecule crystallization using other gels. Recently, Pietras et al. proposed the use of gels based on organic solvents as a new alternative to protein crystallization by counterdiffusion technique. They used polyvinyl alcohol and polyethylene oxide gels to crystallize two model proteins, lysozyme and thaumatine. The quality of the crystals obtained was similar to that of crystals obtained in agar gels by X-ray diffraction [55].

As we emphasized before, controlling the pore size of agarose gels is an intricate task dependent on the nature and concentration of the additives used. Also, because agarose is a natural polymer, impurities and lack of reproducibility can significantly affect the mesh size

[4]. In contrast, the pore size of silica gels is also difficult to control and dependent on the pH and the nature of the reactants used. Conditions under which gel pore size can be controlled often result in a loss of homogeneity along the matrix, and vice versa. Therefore, there is a tradeoff between mesh size and homogeneity in the polymeric matrix.

Because gel mesh size directly affects the rate of diffusion of the precipitating agent, it is important to be able to be able to control it. Mesh size is difficult to control in natural hydrogels such as agar. Therefore, to study the effect of gel mesh size on the crystallization process, synthetic hydrogels are a better alternative. These can be synthesized with control over crosslink density and molecular weight of the precursor polymers. Recently, PEG hydrogels were employed to control nucleation of compounds such as aspirin and acetaminophen [56]. In this work it was demonstrated that the degree of crosslinking could be easily tailored using PEG of different molecular weights. A direct relationship was also found between the molecular weight of the polymer and the mesh size. This resulted in the discovery of an efficient combination that promotes the nucleation process, because the rate of the solute-polymer interaction is controlled [56]. PEG hydrogels are therefore an attractive alternative to control the rate of nucleation of macromolecules.

For these reasons, the use of crosslinked PEG hydrogels to control nucleation, and therefore final crystal size, for the crystallization of macromolecules was proposed. To accomplish this, the technique of counterdiffusion will be employed to combine the benefits of diffusional control by the gel and the physiochemical effects on crystallization due to the geometrical arrangement of the technique.

4 OBJECTIVES

The process of growing protein crystals results in local changes in protein concentration that create density gradients in the protein solution. As a result of these gradients, convective transport is generated under the influence of gravity. This convective transport is responsible for the development of defects and the incorporation of impurities in the protein crystals, which affect their morphology, size, and quality. This effect is undesirable because it renders the crystals unusable for structure determination employing X-ray diffraction, for which high quality crystals are necessary. To obtain high quality crystals, it is therefore desirable that the transport of proteins during the crystallization process be diffusion controlled. One way to ensure this is through the use of gels in the crystallization medium. Among the effect of use of the gel are the suppress of convective mass transport generated by density gradients and the mimicking a microgravity environment. Among the results obtained using gels for protein crystallization was crystal that growth takes place in the three dimensions obtaining full-grown crystal faces. The crystals thus obtained are of bigger size and quality. The most widely used gels for this purpose are agarose and silica for the crystallization of both small and complex molecules. The structure of these gels, however, is difficult to control and there is therefore a lack of information on the effect of the gel structure on the crystallization process. Based on research done for this project, there are no known reports of protein crystallization using gels with a systematic variation of their mesh size in order to limit the convective transport of protein and the precipitating agent and determine its effect on the nucleation process and the size and quality of the crystals. In this context the implementation

of chemically crosslinked PEG hydrogels for controlling macromolecular crystallization using the counterdiffusion technique was proposed. PEG hydrogels allow for control over their structure by varying the polymer concentration. The main objective is therefore to study the effect of the hydrogel structure on the crystallogenesis of proteins and its influence on the size and quality of the crystals. To accomplish this, the following specific objectives will be studied:

- ✓ Characterize the PEG plug hydrogels using the theories of Equilibrium Swelling and Rubber Elasticity.
- ✓ Evaluate the effect of PEG composition in the plug on the transport of the precipitating agent.
- ✓ Investigate the chemical interactions between the hydrogel and model proteins as a function of the polymer concentration.
- ✓ Employ PEG hydrogels to crystallize different model proteins

5 MATERIALS AND METHODS

5.1 MATERIALS

The monomer used was poly(ethylene glycol) monomethyl ether monomethacrylate (#Cat 16666, PEGMA, Polysciences, Warrington, PA) with PEG molecular weights of 1000, poly(ethylene glycol) diymethacrylate ((#Cat 15178, PEGDMA, Polysciences, Warrington, PA) was used as a crosslinking agent and 1-hydroxycyclohexyl phenyl ketone (#Cat 405612, Aldrich Chemical Company, INC, Milwaukee, WI) was selected as the photoinitiator. Both monomers were used as received.

Lysozyme from chicken egg white (#Cat L 6876 Sigma Aldrich, St Louis, MO), Insulin from bovine pancreas (#Cat I-5500 Sigma Aldrich, St Louis, MO), Tris (hydroxymethyl) aminomethane hydrochloride (#Cat T5941 Sigma Aldrich, St Louis, MO), acetic acid glacial (#Cat A0808, Sigma Chemical, St Louis, MO), Ammonium sulphate (#Cat A-4418, Sigma Chemical, St Louis, MO) and sodium acetate (#Cat S-2889, Sigma Chemical, St Louis, MO) were obtained from Sigma. Sodium chloride (#Cat S771-3), Fisher Scientific, Fair Lawn, NJ), Coomassie plus (Thermo Scientific, 3747 N Meridian Rd. Rockford, IL 61101) and Sodium phosphate dibasic (Thermo Scientific, BP332-500 N Meridian Rd. Rockford, IL 61101) were purchased from Fischer Scientific. Glucose Isomerase (#Cat HR7-100 Hampton Research) Agarose (#Cat HR8-092 Hampton Research) were purchased from Hampton Research. HEPES (4-(2-hydroxyethyl)-1-piperazineethanesulfonic acid), (#Cat 11344-041 Gibco® Life Technology Limited, 6482 Carlsbad, CA, Scotland) was obtained from GIBCO

5.2 Methods

5.2.1 Preparation of precipitating agent

For the crystallization of proteins, the use of a precipitating agent that promotes the process of nucleation is needed. The most commonly used agents are salts and organic solvents.

Generally, the precipitating agent is prepared in a buffer specifically prepared for the protein to be crystallized (Table 1). For the crystallization of lysozyme, a buffer of acetic acid and sodium acetate was used (1:10 molar ratio). The buffer was prepared with a concentration of acetic acid/sodium acetate of 0.1 M (pH= 4.6). For the crystallization of insulin, a buffer of 0.1 M Tris(hydroxymethyl)aminomethane hydrochloride (tris/HCL; pH= 9) was employed, and for glucose isomerase, the buffer was 0.1 M 4-(2-hydroxyethyl)-1-piperazineethanesulfonic acid (HEPES; pH= 7). All solutions were dissolved in milli Q water and homogenized using a stirrer. To determine if the solution needed any adjustment, the pH was measured (pH Thermo Orion model 420A). If needed, the pH of the solution was adjusted with 0.1 N hydrochloric acid or 0.1 N sodium hydroxide. The buffers were then passed through a 0.45 μm pore size filter (Fisher Scientific). The precipitating agent was then added at the desired concentration (Table 3). Sodium chloride (.175 M), sodium phosphate dibasic (0.5 M), and ammonium sulphate (0.5-0.8 M) were added to the corresponding buffer for lysozyme, insulin, and glucose isomerase crystallization respectively. The solutions were filtered to remove impurities.

Table 3. The Precipitating agent of proteins

Protein	Buffer	Precipitating agent (buffer)
Lysozyme	0.1M acetic acid/ sodium pH=4.6	Sodium chloride (1.75 M)
Insulin	0.1 M tris/HCL pH= 9	Sodium phosphate dibasic (0.5 M)
Glucose Isomerase	HEPES pH=7	Ammonium sulphate (0.5-0.8 M)

5.2.2 Preparation of protein solution

To study protein crystallization, it is indispensable to have proteins in an environment that allows them to conserve their structural properties. This is often done by solubilizing proteins in buffered mediums where the proteins are stable.

Lysozyme and insulin, supplied as a dry lyophilized powder, were weighed and dissolved in sodium acetate and tris/HCL buffers respectively. Glucose isomerase was supplied as crystals suspended in a buffer solution. The solution was dialyzed for 24 h against Milli-Q water and then for 24 h against 0.1 M HEPES pH 7. The glucose isomerase was then concentrated using a 50 K Amicon Ultra-4 centrifuge and filter device (Millipore). All protein solutions were filtered (0.22 μm) using a sterile syringe (Fisher Brand, MCE, Sterile). The concentrations were checked by measurement absorbance at 280 nm using a molar extinction coefficient using $2.66 \text{ cm}^{-1}\text{mLmg}^{-1}$ for lysozyme , $0.83 \text{ cm}^{-1}\text{mLmg}^{-1}$ for insulin and $0.96 \text{ cm}^{-1}\text{mLmg}^{-1}$ for glucose isomerase with a spectrophotometer (Power Wavex Bio-tek Instruments, Inc.).

5.2.3 Determination of protein concentration in the pre-polymeric solution

A number of colorimetric assays are currently available for the assessment of protein concentration. To quantify the protein, a Coomassie Plus (Bradford) assay kit was used, which required the calibration curve of album as the standard. Before the polymerization a UV spectrophotometer method was used to determine hen-egg white lysozyme protein concentration inside the pre-polymeric solution

Then, a 5 μ L aliquot of the pre-polymeric solution was diluted by a dilution factor of 500 times using sodium acetate buffer. Later, a 10 μ L sample of the last solution was placed in a 96-wells plate (Cat#: 3603, Corning Inc, Corning, NY) with 150 μ L of Coomassie. The blank was 10 μ L of sodium acetate buffer with 150 μ L of Coomassie Plus. The absorbance was determined by a spectrophotometer at 595 nm. (Power wavex Bio-tek Instruments, INC. (Biotech instruments, Inc. Highland Park, Box 998 Winooski, vt 05404-0998 serial no 143379)).

5.2.4 Protein encapsulation in PEG hydrogels, for the determination of the concentration effect

It was found that the counterdiffusion technique in agarose and silica gels worked successfully with a widely range of concentrations of protein models. Some examples are: lysozyme, glucose isomerase and insulin. However, this project dealt with a new hydrogel in the area of protein crystallization. For aforementioned reasons, it was necessary to study this effect on the nucleation process. In this case agarose gel was also used in the protein

chamber in order to compare the results with PEG hydrogel since it has been widely used for this application and its effects on the process are well known.

The monomer monomethyl ether monomethacrylate (PEGMA) 1000 was mixed in a molar ratio of 1:1 with poly-ethylene glycol dimethacrylate (PEGDMA). Both were dissolved in solutions of lysozyme protein at different concentrations, as summarized in table 4. In all cases the hydrogel with 10% w/w was prepared

Table 4. Experimental design

Variable	Levels		
Protein concentration (mg/mL)	40	50	60

Then, a complete dissolution of the components must be achieved by sonication. A photoinitiator (1-hydroxycyclohexyl phenyl ketone) was incorporated in 0.075% w/w of the monomer mixture in the pre-polymeric solution. It was properly sealed, and purged with nitrogen for 20 minutes on an inert glove box (Cole-Parmer, model 34790-40, Vernon Hills, IL), to remove any dissolved oxygen. Dissolved oxygen is known as a free radical scavenger. The solution was loaded across the capillary tube (2.4mm diameter) until the 40 mm long (hydrogel + protein) chamber is filled. The capillary was exposed to a UV source (UV Lamp 100 Watt Mercury Arc, model A4000 EFO Acticure, Canada), for 200 seconds at an intensity of 35 mW/cm². Then, a layer of 5mm of PEG (1000/1000) hydrogel with a molar ratio of 1:1 monomer and cross linker was poured on the top of the previous chamber. For each case, the dissolvent is deionized water, utilized to achieve a prepolymeric solution of 50 % ww/w.

The same procedure was repeated filling the protein chamber with 0.2 % w/v agarose gel. To accomplish this, agarose was weighted and dissolved in a buffer solution (acetic acid/sodium acetate of 0.1 M ; pH= 4.6) to obtain a concentration of 0.4 % w/v . The solution was heated above its fusion temperature ($T_f = 78^\circ\text{C}$) for 20 minutes; then the agarose gel was allowed to cool 10°C above its gelling temperature ($T_g = 24^\circ\text{C}$). This gel was mixed in a volume ratio 1:1 with a protein solution with concentrations of: 80, 100 and 120 mg/mL to obtain a protein chamber of 0.2 % w/v of agarose gel with different protein concentrations (see table 4).

Finally the precipitant solution was added on top of the PEG hydrogel layer to fill the 40 mm long precipitant chamber and then both sides of the capillary tube are sealed using a wax to avoid hydrogel dehydration.

5.2.5 Preparation of counterdiffusion experiments in three layer configuration

PEG hydrogel plugs of different compositions were used to determine their effect on the nucleation process. Experiments were prepared with agarose and PEG hydrogels in the protein chamber. The objective of these experiments was to determine whether plug mesh size could help control the diffusion of the precipitating agent even if different gels were used in the protein chamber.

The monomer poly- ethylene glycol methacrylate (PEGMA) 1000 was mixed in a molar ratio of 1:1 with poly-ethylene glycol dimethacrylate (PEGDMA). Both were dissolved in the

protein solution of lysozyme (70 mg/ mL) corresponding to a hydrogel with 10% w/w. Then, a complete homogenization of the components was achieved by sonication.

A photoinitiator (1-hydroxycyclohexyl phenyl ketone) is incorporated in 0.075% w/w of the monomer mixture in the pre-polymeric solution. It was properly sealed, and purged with nitrogen for 20 minutes on an inert glove box (Cole-Parmer, model 34790-40, Vernon Hills, IL), to remove any dissolved oxygen. Dissolved oxygen is known as a free radical scavenger. The solution was loaded across the capillary tube (4mm diameter) until the 40 mm long (hydrogel + protein) chamber was filled. The capillary was exposed to a UV source (UV Lamp 100 Watt Mercury Arc, model A4000 EFO Acticure, Canada), for 200 seconds at an intensity of 35 mW/cm². Then, a layer of 5mm of PEG hydrogels (1000/1000) was poured on the top of the previous chamber, which a molar ratio of 1:1 monomer and cross linker. For each case, the dissolvent was deionized water, to get pre-polymeric solution with concentrations of 25, 35, 50% w/w of dilution. Again, complete dissolution of the components was achieved by sonication. The processes of homogenization and the addition of the photo-initiator and purge were repeated. Then, the polymerization occurred at different times. These conditions are summarized in table 5

Table 5. Polymerization conditions of the different plug of PEGMA/PEGDMA

Plug PEG composition (%)	Time of UV light exposition (s)
20	80
35	60
50	40

Protein chamber with agarose gel (0.2 % w/v) was prepared as in section 5.4, but keeping constant the protein concentration at 70 mg/mL.

Finally, the precipitant solution was added on top of the PEG hydrogel layer, until filling the 40 mm long precipitant chamber and both sides of the capillary tube are sealed using a wax to avoid hydrogel dehydration.

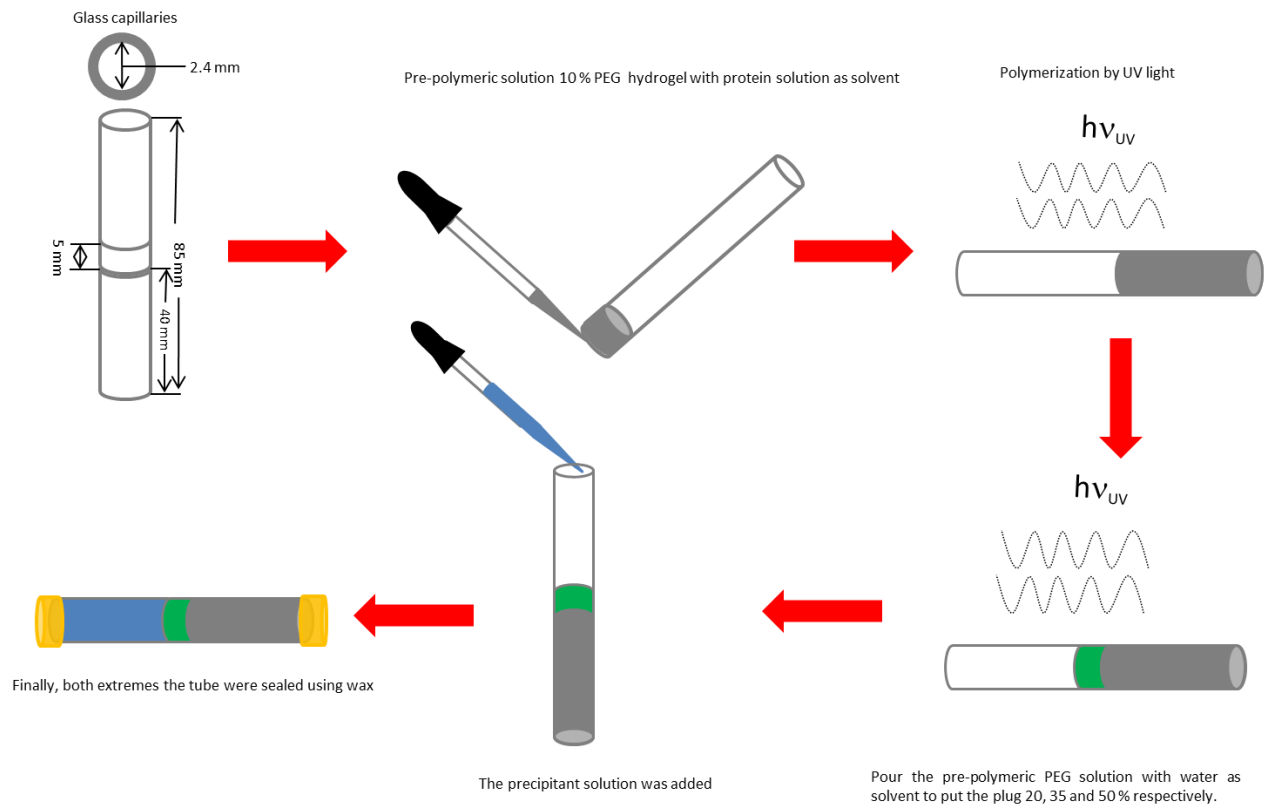


Figure 9. Experimental set up in three Layer configuration

5.2.6 Preparation of capillary counterdiffusion experiments.

The interest was in employing the use of different PEG compositions inside the protein chamber, to evaluate potential protein-gel interactions.

The PEGMA-PEGDMA hydrogels were prepared at 5%, 7%, and 9% mass percent composition of polymer in the pre-polymeric solution. The above percentages consisted of

monomer and cross-linking agent, PEGMA and PEGDMA, mixed at a molar ratio of 1:1. A solution of 40 mg/mL of hen-egg white lysozyme protein was used as the solvent in the pre-polymeric solution. The photoinitiator was incorporated in 0.3% w/w of the monomer mixture. The dissolution was completed using sonication, after which, a homogenous mixture could be observed. It is properly sealed in an amber vial and purged with nitrogen in an inert glove box (Cole-Parmer, model 34790-40, Vernon Hills, IL) for 20 minutes to remove any oxygen. Inside the glove box, the monomer mixture was transferred into 0.8 mm capillary tubes and exposed to a UV source (EXPO, model EFOS Acticure 4000). The conditions are summarized in the next table 6.

Simultaneously, an agarose gel was prepared with a concentration of 0.2 % w/v. The gel was poured inside a Granada crystallization box. Once the agarose was cold the gel was punctured with capillaries. Finally, the precipitating agent was added on top of the gel in 1:1 v/v proportion with respect to the gel.

Capillaries were also prepared for crystallization of insulin and glucose isomerase. In all cases the hydrogels were prepared with an overall PEGMA/PEGDMA concentration of 10 % w/w in the corresponding protein solution. The concentration of insulin was 20 mg/mL and glucose isomerase was used in two concentrations: 30 and 70 mg/mL.

Table 6. Polymerization conditions of the different protein chambers of PEGMA/PEGDMA

PEG composition (%)	Time of UV light exposition (s)
5	600
7	350
9	250
10	200

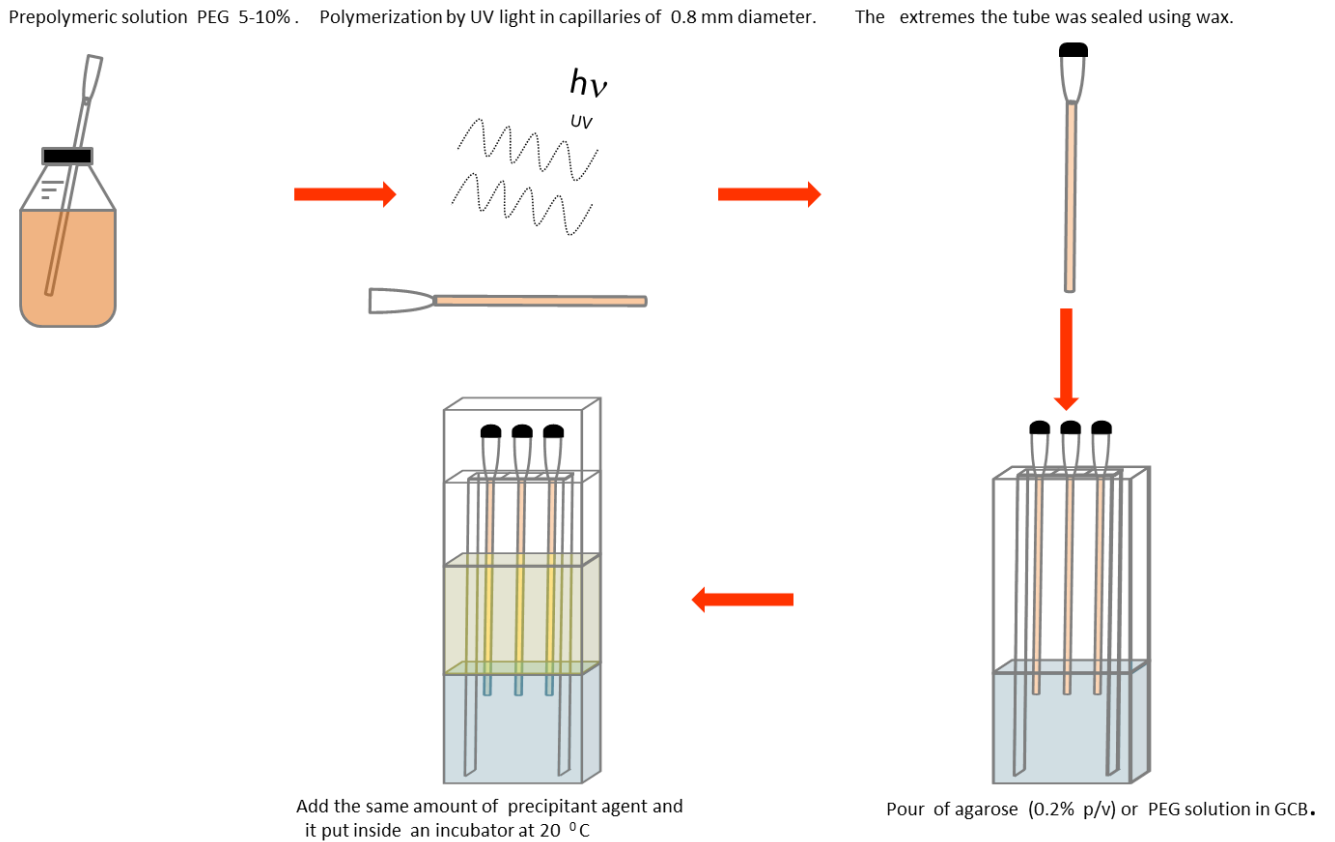


Figure 10. Experimental set up in Granada box crystallization

5.2.7 Determination of nucleation front rate

Transport of the precipitating agent through the protein chamber was studied to determine the effects of the plug composition and the protein concentration. Three different plugs and concentration were used and the advance of the nucleation front through the protein chamber was measured.

Starting when the nucleation process was first observed in the protein chamber, the distance traveled by the nucleation front as a function of time was measured. The distance from the

plug to the nucleation front was measured every 24 hours until the nucleation front reached the end of the protein chamber. Measurements were made a minimum of 3 samples of the same experimental condition. The distance traveled by the nucleation front was found to be proportional to the square root of time except for some samples in which deviations from this linear behavior were observed towards the end of the protein chamber. The linear portion of these data was plotted vs time. The nucleation front rate was obtained from the slope of linear regression fits to the data, which was determined with confidence intervals at 95% for the different variables studied.

5.2.8 Determination of molecular weight of monomers (\bar{M}_{n0})

The average molecular weight of the polymers (\bar{M}_{n0}) was measured by end group analysis from proton Nuclear Magnetic Resonance spectra ($^1\text{H-NMR}$).

Solutions of approximately 10 mg/mL of PEGMA and PEGDMA were prepared using deuterated chloroform. The NMR spectra were obtained on a DRX-500 MHz Bruker spectrometer. Chemical shifts were referenced relative to CHCl_3 at 7.27 ppm. Assignment of peaks to protons of the PEGDMA and PEGMA molecules is reported in figures 12 and 13 respectively.

5.2.9 Raman spectroscopy

Raman Spectroscopy was used to investigate the structure of the prepolymeric solution during the polymerization process. This technique is particularly useful for characterization of hydrogels because the scattering caused by water is negligible. Hydrogels of different

polymer compositions were prepared as described in 5.2.4. The capillaries were placed in the holder of the equipment. The spectra were collected with a time acquisition of 3 s and range of 400-3200 cm^{-1} .

The Raman spectra were recorded with a Renishaw RM2000 and RM1000, equipped with 785 nm laser line (model PI-ECL-785-300-FS, Process Instruments, Inc., Salt Lake City, UT). Laser powers used ranged from: 10 to 60 mW.

5.2.10 Mesh size of PEG hydrogels

The accurate determination of the mesh size provides valuable information for explaining the diffusive velocity of the precipitating agent through the polymeric matrix. To study this effect, hydrogels with different mesh sizes were prepared by the following method:

Equimolar PEGMA-PEGDMA solutions in deionized water were prepared at 20, 35 and 50 mass percent of polymer. Complete dissolution was achieved using sonication. The photo-initiator was then incorporated in 0.075% w/w concentration. The solutions were purged with nitrogen for 20 minutes in an inert chamber. The hydrogels were then prepared by placing the solution between two microslides separated by a Teflon mold held by clamps (Figure 10). The setup was exposed to UV light to initiate the free radical reaction. Different molds were used depending on the test employed to determine the mesh size. Two tests were used: equilibrium swelling and elasticity measurements.

Mesh size by Equilibrium Swelling Theory

Rectangular hydrogel samples (8x4 cm) were prepared using a Teflon mold with 2.4 mm thickness (figure 10). The conditions for hydrogel synthesis are summarized in table 7.

Table 7. Polymerization conditions of the PEG hydrogels for equilibrium swelling characterization.

PEG composition (%)	Time of UV light exposition (s)
20	800
35	350
50	300

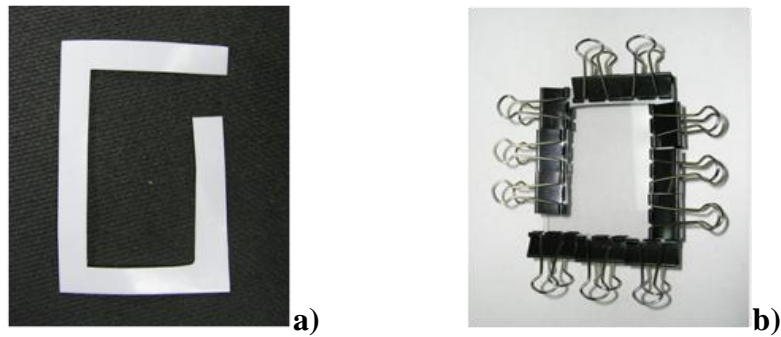


Figure 11. Typical elements to prepare the membranes for determination of the mesh size by equilibrium swelling theory: a) Teflon mold and b) experimental set up.

The hydrogel samples were cut into 9/16" diameter circles immediately after polymerization and their volume was measured using a heptane density kit; the sample was weighed in air (w_a) and then in heptane (w_h) and their difference was related to the volume as shown in eq.

(12) This volume corresponds to the relaxed state (V_r), in order to determine $v_{2,r}$:

$$V_r = \frac{w_a - w_h}{\rho_h} \text{ Eq. (12)}$$

Afterwards, the samples were placed in amber bottles with 15 mL of deionized water and placed in a water bath at 37 °C for three days. The deionized water was replaced three times a day. The volume of the samples was then measured. This volume corresponds to the swollen state (V_s). Finally, the membranes were dried by placing them in a vacuum oven for two days. The volume of the dried samples was then measured (V_d). The measured volumes were used to calculate the volume fraction of polymer in the relaxed and swollen states ($v_{2,r}, v_{2,s}$) as shown below:

$$v_{2,r} = \frac{V_d}{V_s} \text{ Eq. (13)}$$

$$v_{2,s} = \frac{V_d}{V_s} \text{ Eq. (14)}$$

Once obtained these parameters were obtained, the following step was to calculate the molecular weight between crosslinks, \bar{M}_c , using eq. 6 with an assumption: \bar{M}_n is expected to be large given the high molecular weight of the monomer and the high reactivity of acrylate groups, therefore the $\frac{2}{\bar{M}_n}$ term is neglected:

$$\frac{1}{\bar{M}_c} = - \frac{(\bar{v}/V_1)[\ln(1 - v_{2,s}) + v_{2,s} + \chi_1 v_{2,s}] \left[1 + \left(\frac{M_r}{\lambda \bar{M}_c} \right) (v_{2,s}) \right]^3}{\left[(v_{2,s})^{1/3} - \frac{1}{2} v_{2,s} \right] \left[1 - \left(\frac{M_r}{\lambda \bar{M}_c} \right) \left(\frac{v_{2,s}}{v_{2,r}} \right)^{1/3} \right]^2} \text{ Eq. (15)}$$

Here, \bar{v} is the specific volume of the polymer (0.898 cm³/s), V_1 is the molar volume of water (18 cm³/mol), χ_1 is the Flory polymer-water interaction parameter (PEG-water 0.426), λ is the number of links of the monomer after polymerization which to vinyl polymers is two and M_r is the molecular weight of the monomer (1100 g/mol).

The equation was solved by iteration using MathCAD (PTC version 15). The value of \bar{M}_c was then replaced into equation 8 to determine the mesh size:

$$\xi = l v_{2,s}^{-1/3} \left(\frac{2C_n \bar{M}_c}{M_0} \right)^{1/2} \quad Eq. (6)$$

In this expression, ξ is the length of the bond along the backbone chain, C_n is the Flory characteristic ratio of the polymer, and M_0 is the molecular weight of the monomeric repeating units

Mesh size by Rubber Elasticity Theory

Teflon, with 2.4 mm of thickness, was placed between two microslides and held by clamps (See figure 11) The solution was placed in the molds and exposed to UV light. The conditions are summarized in table 8.

Table 8. Polymerization conditions of the membranes of PEGMA/PEGDMA at the same composition of the plug.

PEG composition (%)	Time of UV light exposition (s)
20	800
35	350
50	300

In this case the values of $v_{2,r}$ and $v_{2,s}$ were obtained as was shown above. However, the elasticity modulus of the hydrogel samples was determined from tensile tests performed on an Instron Model 5548 MicroTester with a 10 kN load cell. Custom made adjustable grips with a screw-tightened mechanism were clamped to the sample. The samples were tested in an environmental chamber with DI water kept at a constant temperature of 20 ± 0.1 °C. A constant crosshead displacement rate of 1 mm/min was used for all tests.

Glass beads (30-50 μm) were sprinkled on the surface to use as markers to track the hydrogel deformation. The bead displacements were captured using a Nikon camera and Methamorph software using a time interval of 10 s per frame. For each sample tested, a buoyancy test was done to be included in the calculations.

Once, the value of Young modulus (G) was obtained the value of \bar{M}_c could be determined using equation 7.

$$\bar{M}_c = \left[\frac{\left(\frac{\tau}{\alpha - 1/\alpha^2} \right)}{RTv_{2,s}(\rho 10^6)} + \frac{2}{M_r} \right]^{-1} \quad \text{Where } G = \left(\frac{\tau}{\alpha - 1/\alpha^2} \right) \quad \text{Eq. (7)}$$

In this expression, G , is the Young modulus, τ is the stress applied to the polymer sample, ρ is the density of the polymer M_r is the molecular weight of the initial monomer and α is the deformation ratio (deformed length / initial length).

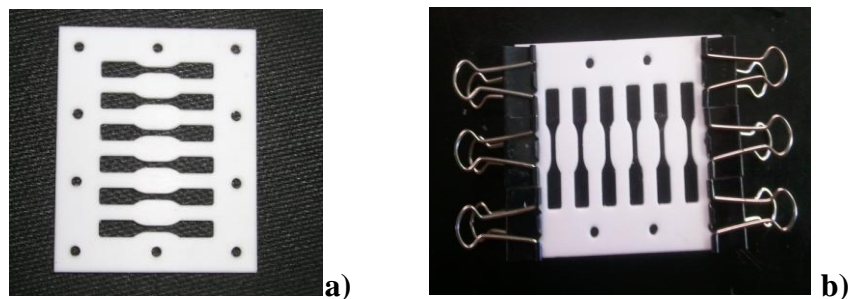


Figure 12. Typical elements to prepare the samples of determination of the mesh size by Rubber Elasticity theory: a) Teflon mold and b) experimental set up.

Finally, the value was substituted into equation 8 to determine mesh size

$$\xi = lv_{2,s}^{-1/3} \left(\frac{2C_n \overline{M}_c}{M_0} \right)^{1/2} \text{ Eq . (8)}$$

The statistical analysis of the results obtained from both methods were done using Minitab 15. Single comparisons were made using an un-paired Student's t-test. Analysis of variance (ANOVA) followed by Tukey's post hoc test was used for data sets with multiple comparisons. A value of $p < 0.05$ was considered significant.

5.2.11 X-ray diffraction

As was previously described, the most adequate technique used to identify the structure of a protein is X-ray diffraction. Once good quality crystals were obtained, it was necessary to prepare them before they were diffracted. In the case of capillaries, once crystal has been selected for diffraction studies, the piece of capillary, where the crystal is found, is isolated

(approximately 1cm) and sealed on both extremes. In the case of crystals contained inside 2.4mm capillaries, the crystals were extracted and cryoprotected with 20%(v/v) glycerol in the crystallization solution. They were soaked for less than 60 s, after which they were placed in a cold nitrogen stream (Kryoflex) maintained at 110 K . Finally, the crystals were placed on the instrument's head and centered using a digital camera that is found aligned on the X-ray plane. X-ray diffraction data were recorded on a Bruker Smart 6000 CCD detector with Kappa configuration (X8 Proteum) using Cu K radiation from a Bruker Microstar microfocus (Montel Optics) rotating-anode generator operated at 45 kV and 60 mA. A total of 483 frames were collected with a 120 s exposure per frame and a crystal-to-detector distance of 70 mm. Integrated intensity information was obtained for each reflection. This was then scaled with SAINT and corrected for absorption with SADABS from the PROTEUM software suite (Bruker AXS Inc.).

6 RESULTS AND DISCUSSION

6.1 Determination of the mesh size

The control of the interactions between protein-precipitating agent in a gel matrix to promote the nucleation process is the one of the most important steps in protein crystallization. These interactions are limited by the velocity of the diffusion front of the precipitating agent through the protein chamber, which is closely related to mesh size. This parameter can be controlled during hydrogel synthesis by, for example, varying the polymer concentration or changing the monomer-to-crosslinker ratio. To determine the operational conditions it was necessary to characterize the plug synthesized using different monomer dilution ratios using the following physical parameters: $v_{2,s}$, $v_{2,r}$, G , χ_1 , among others, of which \bar{M}_c was estimated to obtain the mesh size. \bar{M}_c was calculated using two theoretical methods previously described by equations (6) and (8). However, models for mesh size determination applicable to highly crosslinked gels were used [19]. Figure 13 illustrates the values of the mesh size obtained by two methods. Difference between both methods can be observed. The mesh sizes measured by rubber elasticity varied from 16 to 20 Å, which were larger than those measured by equilibrium swelling. The differences in the mesh size could be a consequence of the nature of the two experiments [57]. One possible explanation for the difference between mesh sizes measured by swelling and those measured by tensile testing is that during the latter some physical entanglements of the polymer chains could be destroyed by the shear exerted during the test, whereas in the swelling measurements the forces on the polymer chains are weaker and entanglements may remain in the structure. This difference

would result in different mesh sizes for the same gel depending on the measurement method. The mesh sizes measured by swelling reflect the state of the hydrogels in the crystallization experiments since no tensile forces are applied. In the case of swelling experiments, the disentanglement process does not occur. For this reason, this type of approach may characterize more accurately the mesh size of the PEG plug employed to control of the precipitating agent [58]. Nevertheless, only in the case of swelling equilibrium was it found that the values of mesh size between 20-35% plug PEG composition did not show statistically significant differences.

The results show that mesh size can be varied by changing the overall polymer concentration of the hydrogel. Even though the mesh size measured by swelling shows no significant difference between the 20 % and 35 % gels, the tensile testing method did show a significant difference. This means that there are structural differences between the two gels that could have an impact on the diffusion of the precipitating agent.

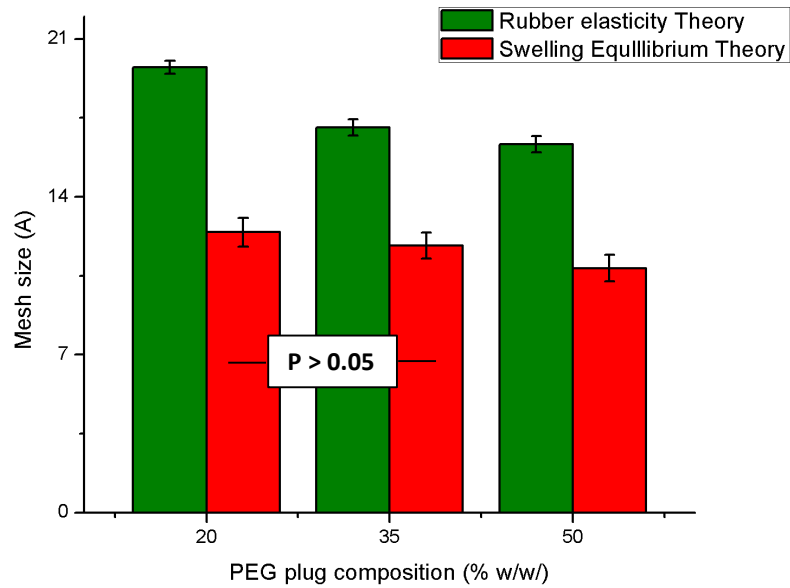


Figure 13. Determination of mesh size of the different PEG plug compositions employed to control diffusion the precipitating agent obtained by equilibrium swelling theory (red bars) and rubber elasticity theory (green bars). Error bars represent standard error of the mean of the mesh size (n= 4 for rubber elasticity method and n=8 for equilibrium swelling). Statistical differences are considered when $p < 0.05$.

6.2 Effect of PEG concentration on the nucleation of lysozyme crystals

Few studies have reported the effects of systematic changes in the gel structure on protein crystal growth. Garcia-Ruiz et al. studied the effect of the concentration of silica gel on the crystals produced by the counterdiffusion technique [59]. However, PEG hydrogels have more flexibility for tailoring the gel structure. This initial study was performed with the purpose of assessing the potential use of PEG-based hydrogels as crystallization substrates. For this purpose, the results obtained by Garcia-Ruiz et al. were utilized as a baseline of comparison to determine whether silica gel and PEG hydrogels could produce similar crystals. Experiments were conducted in capillaries with a diameter of 0.8 mm utilizing different compositions of PEG hydrogel in the protein chamber (The hydrogels prepared in these capillaries were homogeneous and clear) and the plug consisted of 0.2 % w/v agarose. The protein concentration was 40 mg/mL.

Lysozyme protein crystals were successfully grown by the counterdiffusion technique using PEG hydrogels (see figure 16). Nucleation process began 12 hours after the addition of the precipitating agent. The advance of the nucleation front was measured with respect to time until it reached the end of the protein chamber. The nucleation front advance was plotted against the square root of time and in all cases it produced linear trends, which indicated that the transport of the precipitating agent was dominated by diffusion. Figure 14 show this behavior for a concentration of 5% PEG hydrogel in the protein chamber (see appendix 4 for other compositions). Then the data was plotted vs time. The slope of each data set was obtained from a linear regression fit, which corresponds to the nucleation front rate (see

figure 15). Results indicated that as the polymer concentration in the protein chamber was increased the advance of the nucleation front was slower. This is probably due to the slower diffusion of the precipitating agent since as the polymer concentration increased the mesh size of the gel decreased.

It is not common to find changes in crystal morphologies generated by the presence of gels, because the concentrations that were employed usually were low [33, 36, 45]. However, results indicated that different polymer concentrations in the protein chamber induced changes in the morphology of the lysozyme protein crystals formed. The preferential generation of certain crystal morphology is the product of thermodynamic and kinetic parameters governing the processes of crystal growth. As can be observed, (see figure 16 a and b) crystals grown with polymer concentrations of 5 and 7 % w/w showed smooth faces and sharp edges. Therefore, it can be inferred that the crystal growth process followed a two-dimensional mechanism, which consisted of the formation of islands on the surface of the crystal that expanded sideways. Lysozyme crystals have been reported to grow by this mechanism [26, 53].

Crystals grown in 9 % w/w polymer concentration in the protein chamber showed a dendritic structure (see figure 16 c). This type of structure is unstable and can often be the result of irregular distribution of the supersaturation during the formation process. The crystals formed using a polymer concentration of 10% w/w have a spherical shape. The spherical shape of the crystals could be the result of the loss of anisotropic energy of the crystal faces. The dendritic (see figure 19c) and spherical morphologies (see figure 19d) could also be explained by the

normal growth model. When normal growth occurs, protein molecules incorporate into the crystal at rough faces and ordered packaging is difficult. The formation of the crystal is only limited by the adjustment of molecules at the sites of incorporation. [59]. Another possible explanation for the formation of isotropic crystals is that interactions between the precipitating agent and the protein were inhibited by a high polymer concentration because the small mesh size restricted their transport.

As shown, the morphologies of lysozyme crystals evolved from crystals with well-defined faces to crystals with unstable faces to crystals without well-defined vertexes or faces as the concentration of polymer in the gel increases. The crystals begin to show irregularities when the concentration of polymer in the chamber is 9%.

This behavior has been previously observed by Garcia-Ruiz et al. for lysozyme crystals grown in silica gels [59]. They also observed a change from well-defined crystals to spherical crystals as the concentration of the gel was increased. They also found that the crystals grown in high concentration of silica gel were better protected from dehydration. High gel concentration provided mechanical stability to the material while maintaining a humid environment around the crystals. PEG hydrogels are expected to have similar characteristics, since a higher polymer concentration result in a more rigid hydrogel and diffusion of water out of the hydrogel is slower due to smaller mesh size.

Finally, the identity of the lysozyme crystals was confirmed by X- ray diffraction. In this case the parameters used to determine of the quality of crystals was the signal-to-noise ratio[60]. It was found that crystals obtained by the counterdiffusion technique in 9 % and

10 % PEG hydrogel diffracted easily to values near 1.8 Å, this value matches the previous report (1.8-1.9) Å for lysozyme crystals[61]. The results showed that important information about the structure can be obtained through the X-ray diffraction technique (See appendix 3). The use of PEG hydrogel does not appreciably affect the X-ray diffraction quality of the crystal.

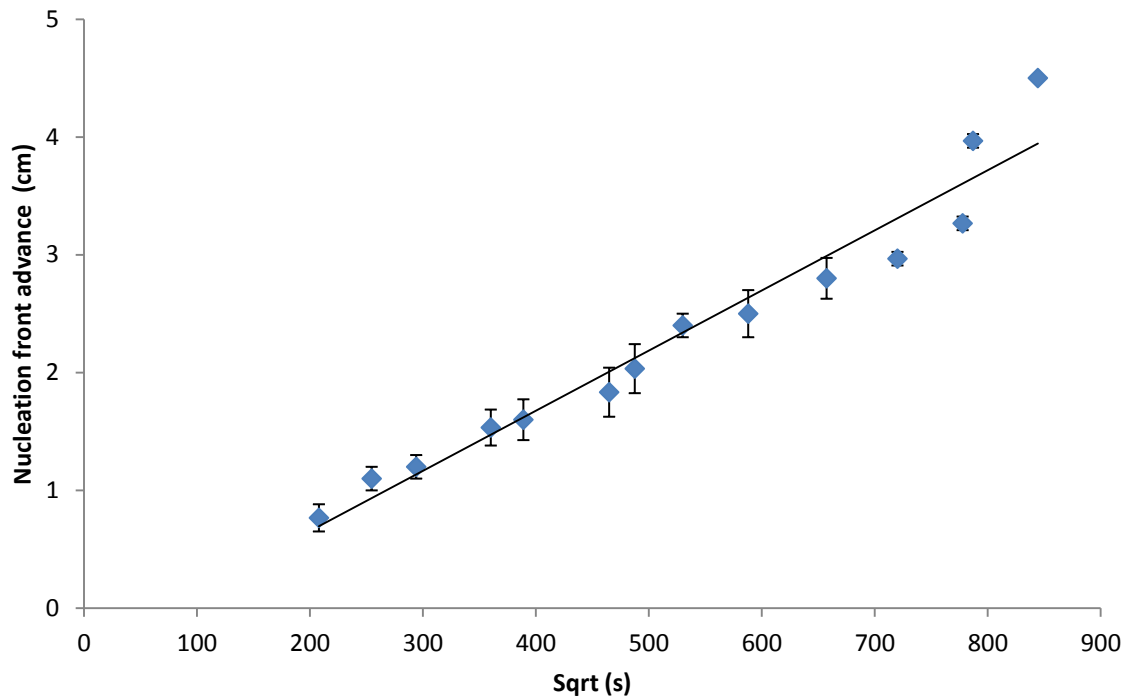


Figure 14 Nucleation advanced front through the protein chamber of 5 % PEG hydrogel prepared with 40 mg/mL protein as a solvent.

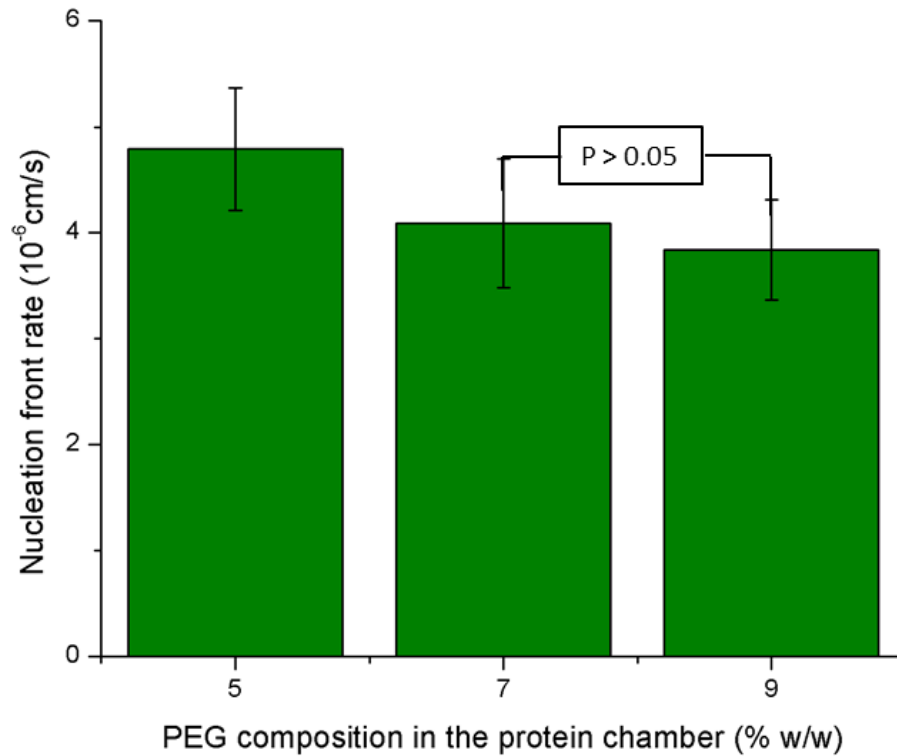


Figure 15 Nucleation front rate of the precipitating agent through the protein chamber with different PEG compositions. Bars represent interval 95 % of confidence for hydrogels. Statistical differences are considered when $p < 0.05$.

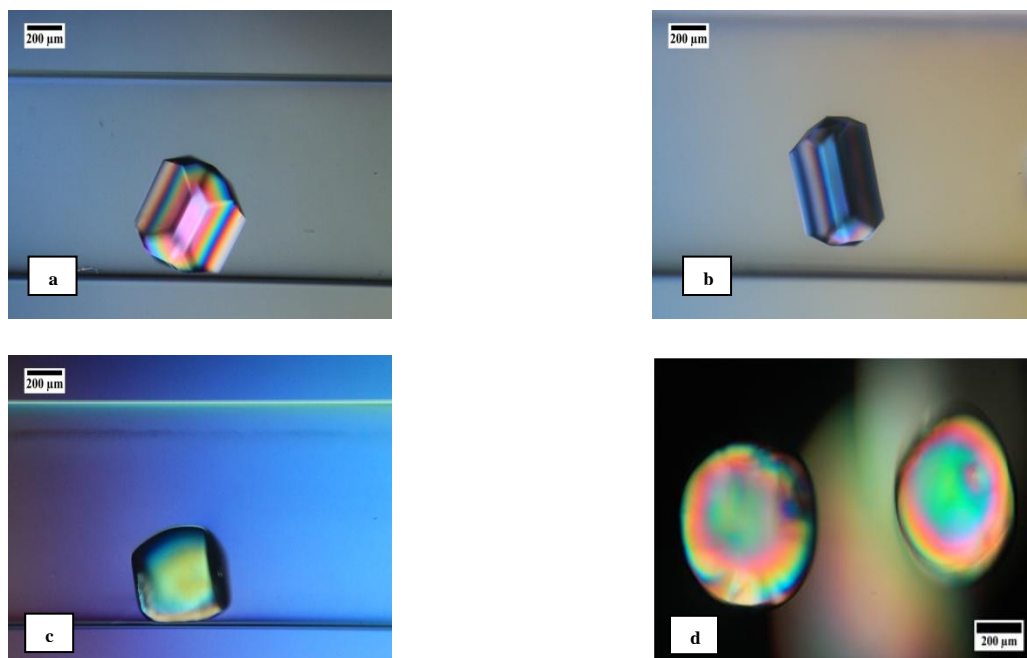


Figure 16. Pictures of lysozyme crystals grown at constant temperature in a PEG hydrogel and different polymer compositions in the prepolymeric solution of: (a) 5% , (b) 7% and (c) 9%, using a 40 mg/mL protein concentration, and (d)10% using a 70 mg/mL protein concentration. The scale bars represent 200 μm .

6.3 Effect of lysozyme protein concentration on the process of nucleation

Since the use of PEG hydrogels for macromolecular crystallization has not been reported, the behavior of the protein inside the hydrogel was studied to determine if the interactions between precipitating agent and protein, which result in dehydration of the protein and crystal growth, were affected. A series of experiments were performed where the concentration of protein was varied while keeping all other parameters constant. The experiments were performed employing the counterdiffusion technique with a three-layer arrangement using tubes of 2.4 mm in diameter as was depicted in section 5.2.4. The plugs consisted of PEG hydrogel prepared at a polymer concentration of 50 % w/w, while the protein chamber hydrogel was prepared with a polymer concentration of 10 % w/w PEG hydrogel. Capillaries with 0.2 w/v agarose gel in the protein chamber were also used for comparison since the effect of this polymer on the crystallization process has been previously reported.

It should be noted that the consistency of the agarose and PEG gels used in this study were very different; the PEG hydrogel was more rigid than the agarose gel. Therefore, there were structural and chemical differences between the two gels that must be mentioned to explain their impact on the crystallization process.

Agarose is a polysaccharide of agarobiose, a dimer of 1,3- β -D-galactopiranosil, 1,4,3,6-anhydro- α -L-galactopiranosil that can present different substituent groups, generally sulphate, pyruvate and methoxy groups (see figure 17) [33]. It is a powder soluble in water

at a temperature of 100 °C. The gelation (T_g) and fusion (T_f) temperatures depend on the percentage of the chemical moieties added to the backbone (sulphate and methyl). Agarose gels are prepared by heating an agarose solution at its fusion temperature (T_f). The mixture is then cooled down below its temperature of fusion (T_g). During the gelation process agarose fibers form double helices which later associate through hydrogen bonding to form a gel structure having hydrophilic properties[38]. The agarose gel is considered a physical gel, because the process of gelation is reversible and chains form physical entanglements rather than chemical. This gel has been employed to evaluate the purity of proteins by electrophoresis as a porous support medium permeated by a buffer solution [26].

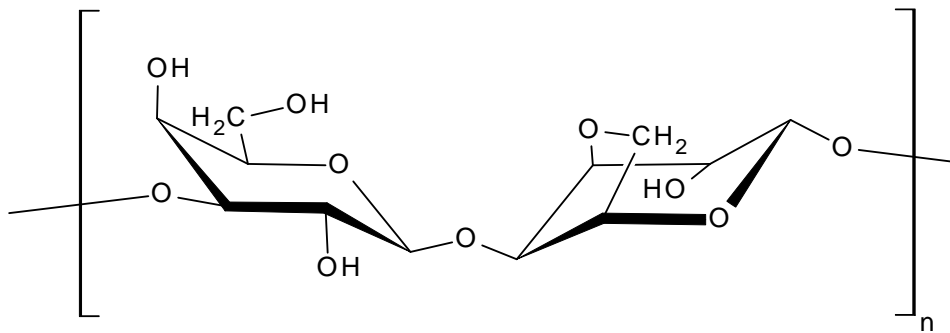


Figure 17 Estructure agarose gel

Agarose gels have been successfully employed as a medium for crystal growth, because it reduces the convective mass transport resulting in high quality crystals to make X-ray diffraction. This hydrogel has many advantages such as: easier preparation and handle, avoids the buoyancy and crystal sedimentation at low concentrations[49] and promotes nucleation without interacting with proteins[52].

PEG, on the other hand, is widely used in the crystallization of macromolecules as a precipitating agent, because it reduces the dielectric properties of the medium promoting specific interactions with proteins that facilitate its crystallization [26]. PEG hydrogels are neutral in nature and are widely used in the biomedical field because of their biocompatibility[8]. The hydrogel used in this research was a crosslinked structure prepared with poly(ethylene glycol) monomethyl ether monomethacrylate and poly (ethylene glycol) di-methacrylate as a crosslinking agent (See figure 18).

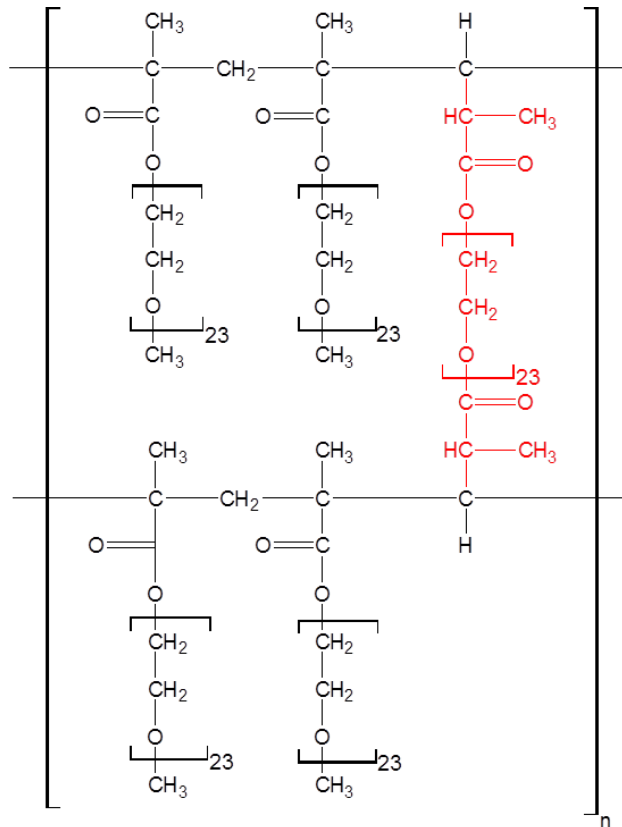


Figure 18 Structure idealized of PEGMA/PEGDMA (1000) hydrogel. Monomer (—) and crosslinker (—).

Both monomers have PEG molecular weights of 1000, which corresponds to 23 repeat units approximately (see figure 18). These monomers contain terminal methacrylate groups that have double bonds, which through polymerization form covalent bonds between each other. A chemically crosslinked hydrogel was obtained by radical polymerization in the presence of crosslinking agent.

Nucleation process began 48 and 72 hours after the addition of the precipitating agent when the gel in protein chamber was agarose and PEG respectively. The advance of the nucleation front was measured with respect to time until it reached the end of the protein chamber. The nucleation front advance was plotted against the square root of time.

Figure 19 shows that the nucleation front advance along the protein chamber with PEG hydrogels was faster than with agarose gel. This behavior could be explained by the effect of the mesh size on the diffusion of the precipitating agent or by the interactions between the gel and the protein, which may have an effect on the nucleation process. The mesh size of the PEG hydrogel in the protein chamber (10% hydrogel) was measured at 42.45 Å (determined using the swelling equilibrium theory), which is much smaller than that of the agarose gel (0.2 % w/v) 2300 Å. (determined using a plot of the Rigetti correlation, which shows agarose concentration vs mesh size [33]). From the size differences one would expect that the precipitating agent would diffuse faster in the agarose gels and, therefore, the nucleation front would advance at a faster rate than in the PEG hydrogel. For this reason, the possible nucleation promoting effect of the PEG hydrogel on lysozyme must be considered. It is well

known that agarose gel is a promoter of nucleation. When the protein concentration was increased to 50 mg/ml (see figure 20) the nucleation rate advance in the PEG hydrogel was faster than in agarose but it was similar in the final zone of the protein chamber. Finally, at 60 mg/ml protein concentration the nucleation front advance was faster in the agarose gel when is compared with the PEG hydrogel (see figure 21). The results indicated that a higher concentration of protein allows the system to reach the supersaturation state faster in agarose due to the dehydration effect of the precipitating agent on the protein. This effect of nucleation promotion was observed when the protein chamber was filled with PEG hydrogel with respect to agarose gel at low protein concentrations. The reduction in nucleation promotion in the PEG hydrogel with increasing protein concentration might be explained by nonhomogeneous polymerization when the solution was exposed to UV light.

Moreover, in all cases no differences were observed in the crystal structure or size as a function of distance from the plug, but there were differences between crystals grown in PEG and those grown in agarose. Photos obtained from polarized light microscopy showed that the crystals grown in the PEG hydrogel were spherical regardless of the concentration of protein used (figure 22). This morphology is not commonly found in the crystallization of macromolecules [34]. The lysozyme crystals grown in agarose gels are show in figure 23.

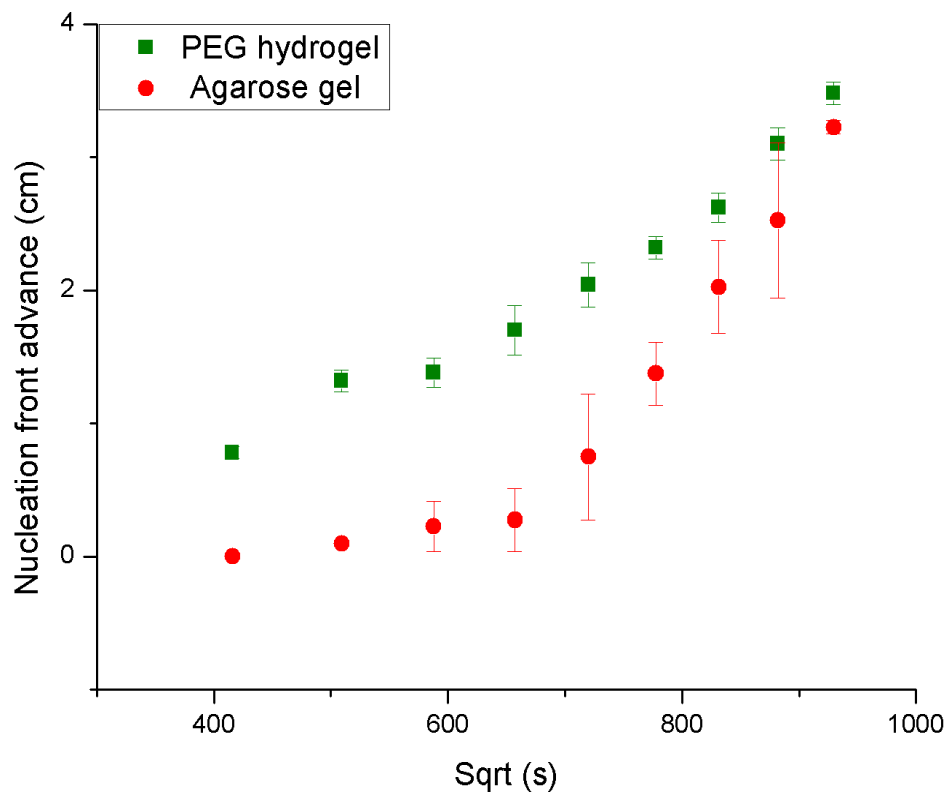


Figure 19 Nucleation front advance vs. square root time. The hydrogels were prepared with a protein concentration of 40 mg/mL.

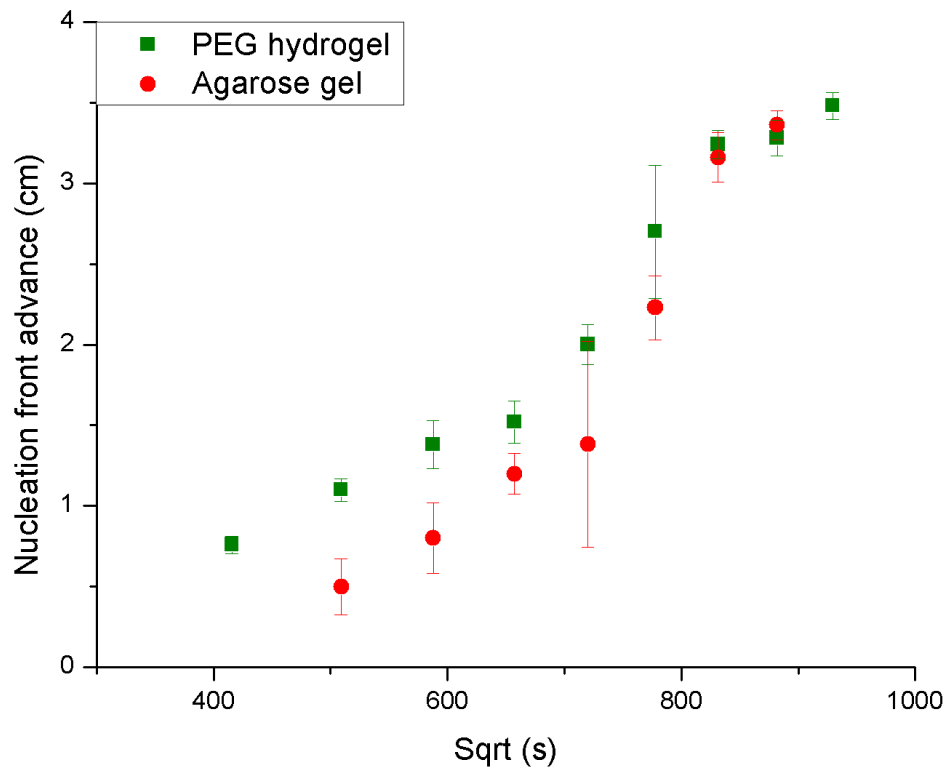


Figure 20 Nucleation front advance vs. square root time. The hydrogels were prepared with a protein concentration of 50 mg/mL.

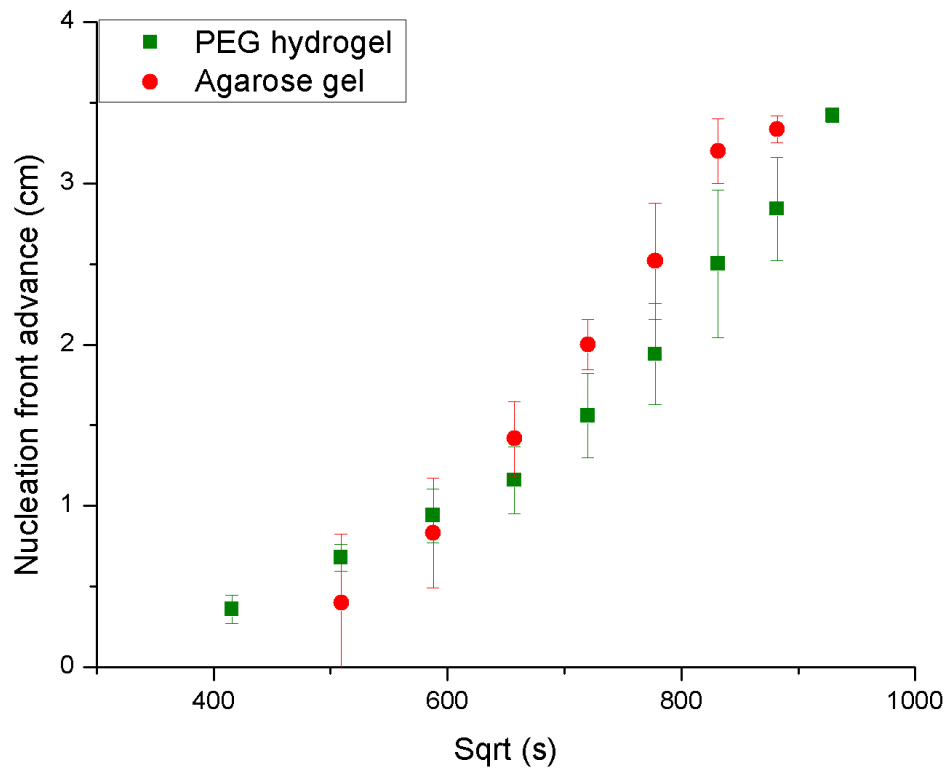


Figure 21 Nucleation front advance vs. square root time. The hydrogels were prepared with a protein concentration of 60 mg/mL

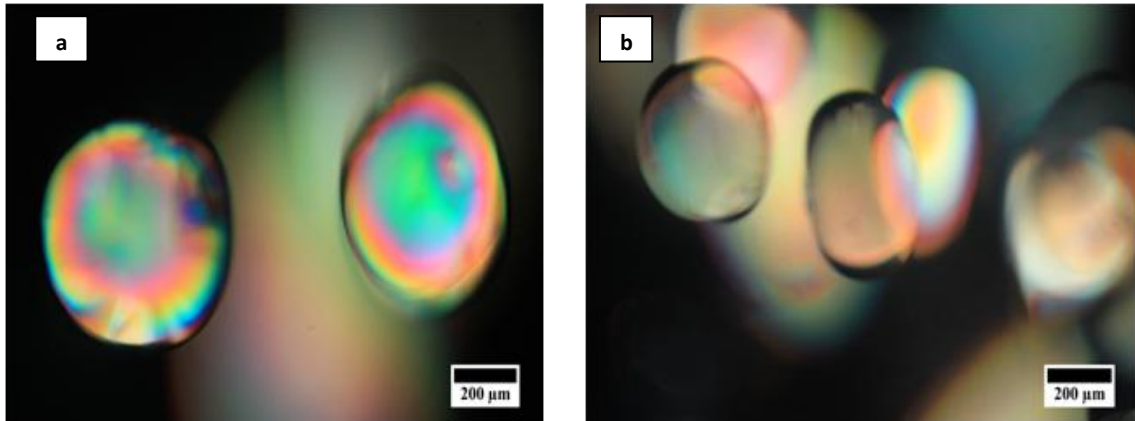


Figure 22. Pictures of lysozyme crystals grown at constant temperature in a 10% PEG hydrogel using protein concentration of: (a) 40 mg/mL (b) and 60 mg/mL. The scale bars represent 200 μm .

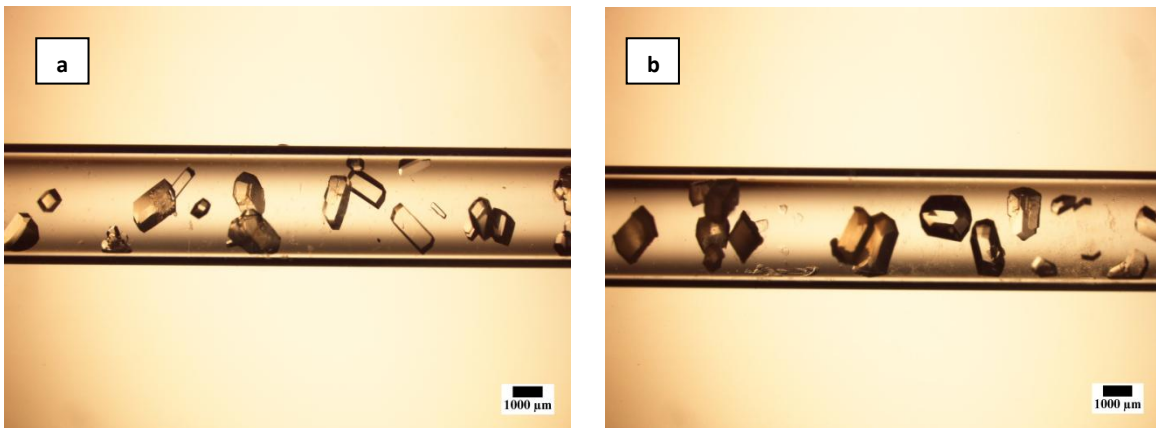


Figure 23 Pictures of lysozyme crystals grown at constant temperature in a 0.2 (w/v) agarose gel using protein concentration of: (a) 40 mg/mL (b) and 60 mg/mL. The scale bars represent 1000 μm .

6.4 Effect of the plug composition on the supersaturation wave

The 3-layer arrangement of the counterdiffusion technique was developed to attain finer control over the development of the supersaturation wave to obtain high quality crystals. Although this experimental setup has been successfully used for the crystallization of small and complex molecules, no studies have been reported on the effect of the plug mesh size on the diffusion of the precipitating agent. Agarose and silica gels, the most widely used hydrogels for protein crystallization, are not appropriate for this type of study since their structural properties cannot be easily manipulated. In contrast, chemically crosslinked hydrogels allow control of their structural properties by varying the monomer to crosslinker ratio and their overall concentrations. Therefore, the synthesis of PEG hydrogel plugs with systematic variation of the mesh size by changing the overall polymer concentration was proposed. These plugs in the 3-layer counterdiffusion setup and their effect on the nucleation and crystallization process was observed. For this study 2.4 mm capillaries, as described in section 5.2.4, were used. The capillaries were fitted with PEG hydrogel plugs prepared with polymer concentration of 25, 35, and 50 % w/w. The protein concentration in all experiments was held at 70 mg/mL. Experiments were performed filling the protein chamber with agarose gel (0.2 % w/v) or PEG hydrogel with 10 % w/w polymer concentration. The time was measured until the first nucleation events were observed and the advance of the nucleation front in the protein chamber.

Differences were found in the time at which nucleation was first observed as a function of plug composition irrespective of the gel used in the protein chamber. As expected, the first nucleation events were observed at later times as the mesh size of the plug decreased.

When using PEG hydrogel in the protein chamber, the initial nucleation events in the gel were observed at 24, 48 and 72 hours for the systems using plugs with compositions of 20, 35, and 50 % w/w. Two crystallization zones in the protein chamber were observed. At the beginning of the protein chamber, near the plug, polycrystalline precipitates were formed due to the high level of supersaturation present in this zone. This type of precipitate was formed in the first 10 mm of the protein chamber. From this point on, the formation of many small crystals was observed. There was no variation in crystal size along the remainder of the protein chamber (see figure 24). The nucleation front advance was proportional to the square root of time, which is indicative of diffusive transport of the precipitating agent through the protein chamber (see appendix 5). The nucleation front rate constant was higher for the 20 % polymer composition and similar for 35 and 50 % compositions (see figure 26).

In the case of protein chambers filled with agarose gels the times for initial nucleation were 24, 36 and 48 hours for the systems using plugs with compositions of 20, 35, and 50 % w/w. However, large crystals (ca. 800 μm) formed along the whole protein chamber with larger crystals being obtained when using the plug with the smaller mesh size (see figure 25). Additionally, the nucleation front advance was initially proportional to the square root of time, but at a certain point it deviated from this behavior advancing at a faster rate with time

(see appendixes 6). The slope of the linear region was obtained from linear regression fits to obtain the nucleation front rate constant (See figure 26).

The results showed that it is possible the control of final size of the crystal simply through changes in PEG composition in the plug. However, it is necessary to determine whether the large crystals formed in agarose are of polycrystalline nature or single crystals to know which gel produces crystals of higher quality. In the case of the PEG hydrogels, several parameters can be changed: for example, the length of the protein chamber and the polymer concentration.

The Grashof number, which is the ratio of the buoyancy forces and viscous forces acting on a fluid, can be used to determine whether the process of convective mass transport is reduced by using PEG plugs of different compositions to control of the diffusion of precipitating agent. The Grashof number is given by[7]

$$N_G = \frac{g\rho\left(\frac{\delta\rho}{\delta c}\right)\Delta c d^3}{\mu^2}$$

Where: g is the gravitational acceleration, ρ is the density of the fluid, $(\delta\rho/\delta c)$ is the density increase with concentration of solute, Δc is the solute concentration difference present in the system, d is the characteristic dimension of the system, and μ is the viscosity of the fluid. From the definition of the Grashof number it is possible to identify the variables that may help reduce the buoyancy forces that promote natural convection transport with respect to diffusion. The most effective way to reduce N_G is to perform the experiments

in microgravity conditions, effectively reducing g , but this is very expensive. A second option is to increase the viscosity of the fluid by adding a thickening agent, but the possible interference of this agent with the crystallization process must be considered. Finally, reducing the characteristic length of the system will have a large effect given that it is elevated to the third power. In the capillaries the characteristic lengthscale is the diameter of the tube, but by employing the gel the characteristic lengthscale is of the order of the mesh size. The absolute value of N_G cannot be calculated since the concentration difference is unknown, but considering that conditions are similar for all the plugs used, one can calculate the relative values of N_G for the different plugs as shown in table 9.

Table 9 Ratio of the Grashof number among different PEG plug compositions

Mesh size (Å)	Ratio PEG plug compositions (% w/w)	Grashof number ratio
20% = 12.43	20 - 35	$N_G 20\% = 1.16 N_G 35\%$
35% = 11.84	20-50	$N_G 20\% = 1.5 N_G 50\%$
50% = 10.84	35-50	$N_G 35\% = 1.3 N_G 50\%$

The calculations show that $N_{G,20\%}$ is 50 % larger than $N_{G,50\%}$ and 16 % larger than $N_{G,35\%}$; while $N_{G,35\%}$ is 30 % larger than $N_{G,50\%}$. This means that as the polymer concentration is increased N_G becomes smaller and, therefore, viscous forces dominate over buoyancy forces. Given that convection in the crystallization experiments performed is only

caused by buoyancy forces, it will be limited more effectively at higher polymer concentrations.



Figure 24. Pictures of lysozyme crystals grown at constant temperature in a 10% PEG hydrogel using PEG plug composition of 20% in different zones of the capillaries: (a) initial, (b) medium and (c) final. The scale bars represent 200 μm.

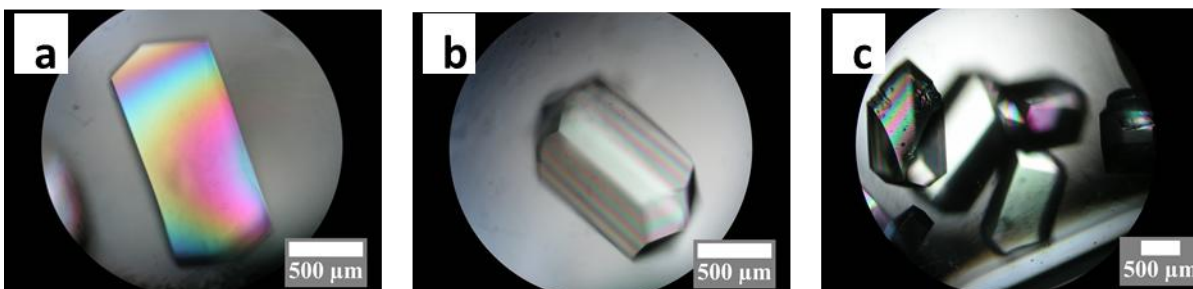


Figure 25. Pictures of lysozyme crystals grown at constant temperature in a 0.2% (%w/v) agarose using different PEG plug composition: (a) 20 , (b) 35 and (c) 50% respectively. The scale bars represent 500 μm.

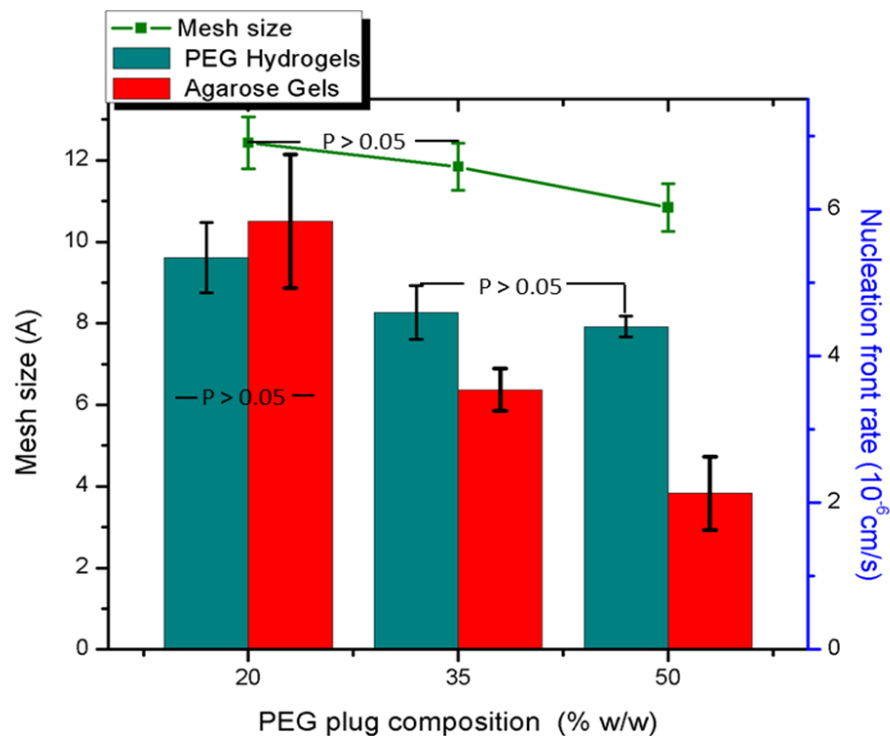


Figure 26. Nucleation front rate of the precipitating agent through the protein chamber (10%) PEG hydrogel and agarose gel (0.2 % w/v) for each employed PEG plug and its respective mesh size obtained by equilibrium swelling. Bars represent interval 95 % of confidence for hydrogels. In the case of mesh size the bars represent the standard deviation. Statistical differences are considered when $p < 0.05$.

6.5 Hardware prototype for the control for the control of precipitating agent diffusion using ad hoc PEG-Plugs

Since the protein-gel interaction is inevitable during mixing in the protein chamber and its influence on the crystallization will depend on the nature of the protein, the easiest way to control the diffusion of the precipitating agent without changing the protein environment is by varying the plug mesh size.

The previous results indicate that it is possible to control the diffusion of the precipitating agent employing PEG plugs of different mesh size. This could facilitate macromolecule crystallization experiments. For example, a series of crystallization conditions can be explored varying the plug mesh size to induce different diffusion conditions. Commercialization of capillaries with plugs of specific mesh size is possible using the prototype shown in figure 27. This prototype would work under the principles of the counterdiffusion technique using a three layer arrangement. This device consists of capillaries of appropriate length in which plugs with different mesh sizes and/or lengths are formed to offer different options. The protein chamber has a fixed length and the precipitating agent chamber changes according the length of the PEG plug employed. To preserve the plug and avoid dehydration the protein and precipitating agent chamber would be filled with water and both extremes sealed with adjustable rubber stoppers

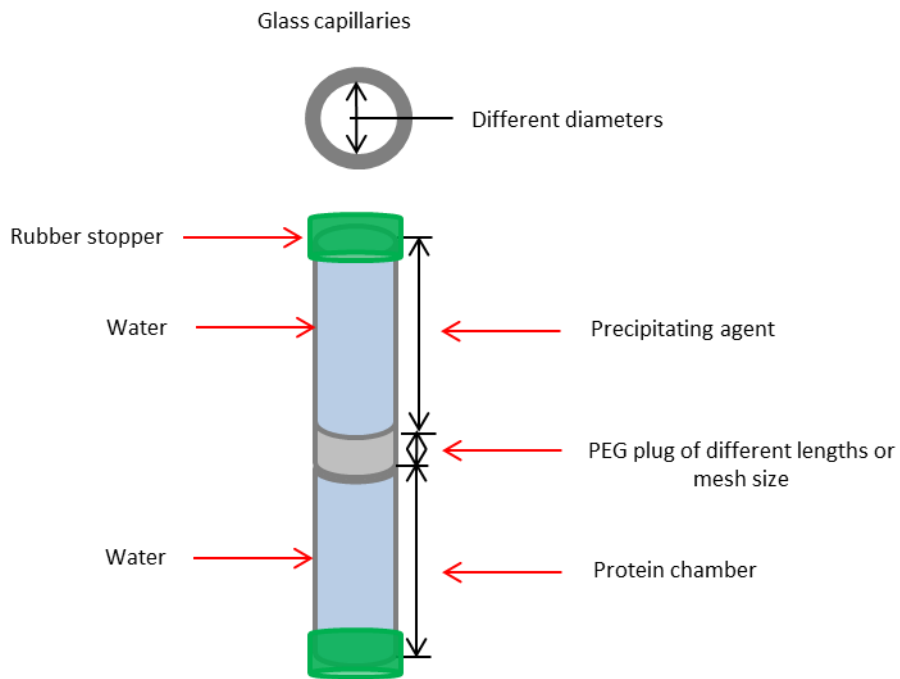


Figure 27 Device to crystallize macromolecules based on the principle of counterdiffusion using a three layer arrangement

6.6 Generalization of the use of PEG hydrogels in crystallization

While lysozyme crystallization using PEG hydrogels was demonstrated, it would be useful to show the applicability of these gels for crystallization of other types of proteins. To this end, two other proteins were crystallized in PEG hydrogels: insulin and glucose isomerase. To perform these experiments the 3 layers counterdiffusion arrangement was used with capillaries of 0.8 mm in diameter. The capillaries were punctured in agarose (0.2 % w /v) which served the function of a physical buffer inside a Granada Crystallization Box (See section 5.2.6).

Insulin was successfully crystallized for the first time in PEG hydrogels. We observed the first crystals 8 days after the experiment was set up (see figure 28). The crystals that were obtained had morphology similar to those obtained by other techniques such as sitting drop crystallization [62]. A systematic study of the crystallization process is still needed, but the limited availability of the protein prevented us from doing it at this time.

In the case of glucose isomerase, crystallization in PEG hydrogels was successful although the appearance of the first crystals, which had needle-like morphology, took 45 days, similar morphology was obtained by batch method (see figure 29) [63]. Additionally, dehydration of the gel was also observed; this was attributed osmotic dehydration; the salt $((\text{NH}_4)_2\text{SO}_4)$ employed could reduce the swelling capacity of the hydrogel, which results on phase separation and dehydration of the gel [64]. The concentration of the precipitating agent was therefore decreased and that of the protein was increased to maintain supersaturation conditions, while avoiding dehydration of the gel. These changes resulted in a reduction in

the time for crystal formation and change in their morphology. The first crystals were observed after only 10 days and had a faceted morphology (See figure 30), which has been previously obtained by counterdiffusion[36].

The usefulness of PEG hydrogels for the crystallization of a variety of proteins has therefore been demonstrated. In the future, it will be interesting to study whether the specific interactions between PEG hydrogels and certain types of proteins aid in their crystallization. In addition, PEG hydrogels may aid in the crystallization of other types of proteins that present a challenge in their crystallization, such as membrane proteins.

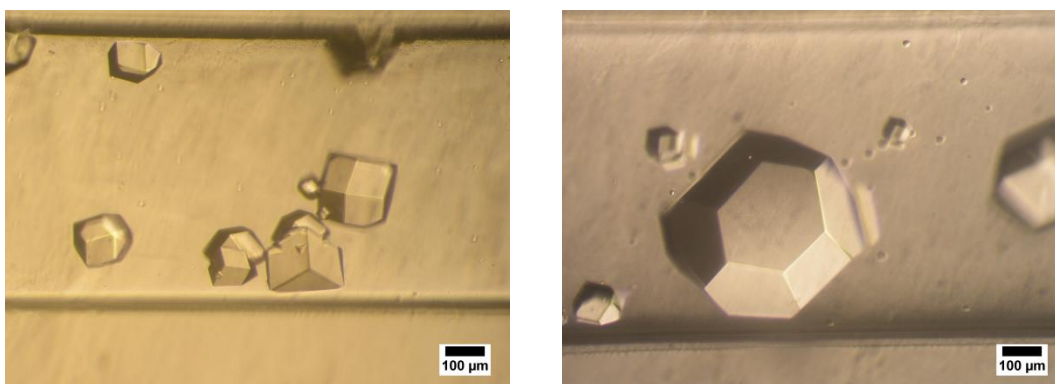


Figure 28 Pictures of insulin crystals grown at constant temperature in a 10% PEG hydrogel using protein (20mg/mL) as a solvent. The scale bars represent 100 µm.

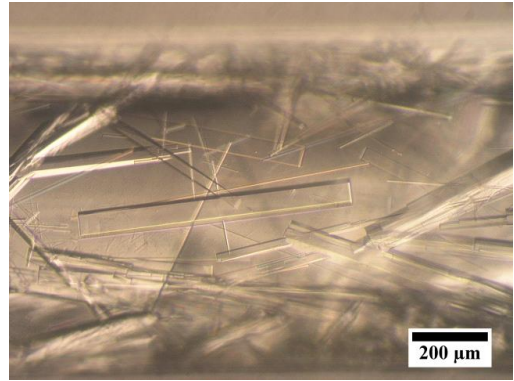
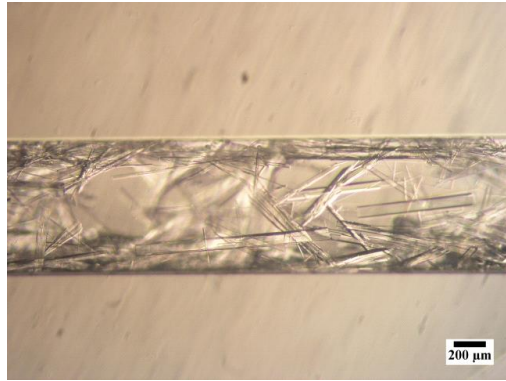


Figure 29 Pictures of glucose isomerase crystals grown at constant temperature in a 10% PEG hydrogel using protein solution (30mg/mL) as a solvent. The scale bars represent 200 μm

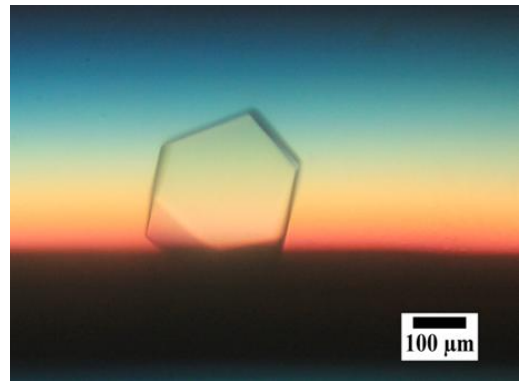
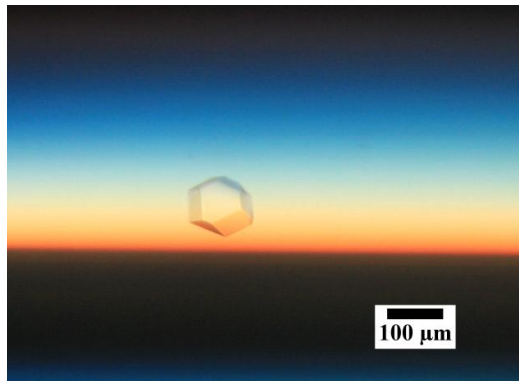


Figure 30. Pictures of glucose isomerase crystals grown at constant temperature in a 10% PEG hydrogel using protein solution (70mg/mL) as a solvent. The scale bars represent 100 μm .

7 CONCLUSIONS

The growth of protein crystals in gels has great potential for obtaining high quality crystals that can be used to resolve their structures. This is important in many areas such as biotechnology and pharmaceuticals. The vast majority of protein crystallization studies have used agarose and silica as gels. The systematic study of other gels for the crystallization of macromolecules has the potential to allow us to better understand the process and it would be a significant contribution to the scientific community.

Our contribution in this area consists of the implementation of PEG hydrogels to crystallize macromolecules. This type of gel can be synthesized under different conditions and characterized to determine its mesh size. We observed changes in the diffusion rate of the precipitating agent as a result of the differences in mesh size of the PEG gel in the protein chamber. The results confirmed the hypothesis that the crystallization process could be controlled using PEG hydrogels.

It was demonstrated that PEG hydrogels could be used to grow lysozyme protein crystals. Increasing the polymer concentration in the protein chamber delayed the process of nucleation, which is due to the decrease of mesh size of the hydrogels. Also, the restriction exerted by the rigidity of the hydrogel when the polymer concentration increases disrupts anisotropic growth of the crystal faces resulting in spherical crystals similar to those obtained using silica gels.

One of the most relevant results was that X-ray diffraction demonstrated that the quality of the crystals was not affected by employing PEG hydrogels compared to crystals grown in

solution. Whether the crystal quality was improved will have to be determined by neutron crystallography.

The increase of lysozyme protein concentration decreased the effect induction of nucleation process of the PEG hydrogels when is compared with agarose gels. This is a preliminary result that merits further study. The interactions between the hydrogel and the protein can be studied by techniques small angle neutron scattering or X-ray scattering. These interactions can then be correlated to their effect on the nucleation process.

The use of PEG hydrogel plugs allows for the control the diffusion process of the precipitating agent. The plug mesh size can be adjusted to afford control over the evolution of the saturation front and over the crystal size for neutron crystallography. In this manner, it was possible to control the nucleation process without interfering with the protein.

Finally, the wide applicability of PEG hydrogels for protein crystallization was demonstrated. Crystals of different proteins employing the three layer configuration with counterdiffusion Gel Acupuncture Method (GAME) were obtained with good crystal quality.

8 REFERENCES

1. McPherson, A., *Introduction to protein crystallization*. Methods (Oxford, United Kingdom), 2004. **34**(3): p. 254-265.
2. Mirkin, N. and A. Moreno, *Advances in Crystal Growth Techniques of Biological Macromolecules*. J. Mex. Chem. Soc, 2005. **49**(1): p. 39-52.
3. Otalora, F., et al., *Counterdiffusion methods applied to protein crystallization*. Progress in Biophysics and Molecular Biology, 2009. **101**(1-3): p. 26-37.
4. Lorber, B., et al., *Crystal growth of proteins, nucleic acids, and viruses in gels*. Progress in Biophysics and Molecular Biology, 2009. **101**(1-3): p. 13-25.
5. Robert, M.C. and F. Lefauchaux, *Crystal growth in gels: Principle and applications*. Journal of Crystal Growth, 1988. **90**(1-3): p. 358-367.
6. Langer, R. and N.A. Peppas, *Advances in biomaterials, drug delivery, and bionanotechnology*. AIChE Journal, 2003. **49**(12): p. 2990-3006.
7. Garcia-Ruiz, J.M., J. Charles W. Carter, and R.M. Sweet, *Counterdiffusion Methods for Macromolecular Crystallization*. Methods in Enzymology, 2003. **368**: p. 130-154.
8. Cai, W. and R.B. Gupta, *Hydrogels*, in *Kirk-Othmer Encyclopedia of Chemical Technology*. 2002, John Wiley & Sons, Inc.
9. Peppas, N.A., et al., *Physicochemical Foundations and Structural Design of Hydrogels in Medicine and Biology* Annual Review of Biomedical Engineering, 2000. **2**(1): p. 9-29.

10. Saul, J.M. and D.F. Williams, *Hydrogels in Regenerative Medicine*, in *Principles of Regenerative Medicine*. 2011, Academic Press: San Diego. p. 637-661.
11. Dang, J.M. and K.W. Leong, *Natural polymers for gene delivery and tissue engineering*. *Advanced Drug Delivery Reviews*, 2006. **58**(4): p. 487-499.
12. Gerlach, G. and K.F. Arndt, eds. *Hydrogels Sensor and Actuators*. Series on Chemical Sensors and Biosensors, ed. G. Urban. Vol. 6. 2010, Springer: Berlin.
13. Corkhill, P.H., C.J. Hamilton, and B.J. Tighe, *Synthetic hydrogels VI. Hydrogel composites as wound dressings and implant materials*. *Biomaterials*, 1989. **10**(1): p. 3-10.
14. Topuz, F., et al., *Hydrogels in Biosensing Applications*, in *Comprehensive Biomaterials*, P. Ducheyne, Editor. 2011, Elsevier: Oxford. p. 491-517.
15. Baldwin, A.D. and K.L. Kiick, *Polysaccharide-modified synthetic polymeric biomaterials*. *Peptide Science*, 2010. **94**(1): p. 128-140.
16. Singh, A., et al., *Hydrogels: a Review*. *Int. J. Pharm. Sci. Rev. Res.*, 2010. **4**(2): p. 97-115.
17. Peppas, N.A., et al., *Hydrogels in Biology and Medicine: From Molecular Principles to Bionanotechnology*. *Advanced Materials*, 2006. **18**(11): p. 1345-1360.
18. Lowman, A.M. and T.D. Dziubla, *Gels*, in *Encyclopedia of Smart Materials*. 2002, John Wiley & Sons, Inc.
19. Peppas, N., A., *Fundamentals*, in *Hydrogels in Medicine and Pharmacy*. 1987, CRC Press, Inc. Boca Raton, Florida.

20. Slaughter, B.V., et al., *Hydrogels in Regenerative Medicine*. *Advanced Materials*, 2009. **21**(32-33): p. 3307-3329.
21. Cruise, G.M., D.S. Scharp, and J.A. Hubbell, *Characterization of permeability and network structure of interfacially photopolymerized poly(ethylene glycol) diacrylate hydrogels*. *Biomaterials*, 1998. **19**(14): p. 1287-1294.
22. Lowman, A.M. and N.A. Peppas, *Analysis of the Complexation/Decomplexation Phenomena in Graft Copolymer Networks*. *Macromolecules*, 1997. **30**(17): p. 4959-4965.
23. Beamish, J.A., et al., *The effects of monoacrylated poly(ethylene glycol) on the properties of poly(ethylene glycol) diacrylate hydrogels used for tissue engineering*. *Journal of Biomedical Materials Research Part A*, 2009. **92A**(2): p. 441-450.
24. Canal, T. and N.A. Peppas, *Correlation between mesh size and equilibrium degree of swelling of polymeric networks*. *Journal of Biomedical Materials Research, Part A*, 1989. **23**(10): p. 1183-1193.
25. Feigelson, R.S., *The relevance of small molecule crystal growth theories and techniques to the growth of biological macromolecules*. *Journal of Crystal Growth*, 1988. **90**(1-3): p. 1-13.
26. McPherson, A., *Crystallization of Biological Macromolecules*. 1999: Cold Spring Harbor Laboratory Press, Cold Spring Harbor.

27. Ng, J.D., J.A. Gavira, and J.M. Garcia • a-Ruiz, *Protein crystallization by capillary counterdiffusion for applied crystallographic structure determination*. Journal of Structural Biology, 2003. **142**(1): p. 218-231.
28. Ducruix, A. and R. Giege, eds. *Crystallization of Nucleid Acids and Proteins: A Practical Approach*. The Practical Approach Series, ed. B.D. Hames. 1999, Oxford University Press: New York.
29. McPherson, A., *Introduction to Macromolecular Crystallography*. 2009: John Wiley & Sons, Press.
30. Beamish, J.A., et al., *The influence of RGD-bearing hydrogels on the re-expression of contractile vascular smooth muscle cell phenotype*. Biomaterials, 2009. **30**(25): p. 4127-4135.
31. Ulrich, J. and T. Stelzer, *Crystallization*, in *Kirk-Othmer Encyclopedia of Chemical Technology*. 2011, John Wiley & Sons, Inc.
32. Garcia-Ruiz , J.M., *Nucleation of protein crystals*. Journal of Structural Biology, 2003. **142**(1): p. 22-31.
33. Gavira, J.A., *Cristalizacion de Proteinas en Geles por Metodos Contradifusivos*, in *Chemistry*. 2000, Universidad de Granada, Spain.
34. Vekilov, P.G., *Nucleation*. Crystal Growth & Design, 2010. **10**(12): p. 5007-5019.
35. DeLucas, L.J., et al., *Efficient protein crystallization*. Journal of Structural Biology, 2003. **142**(1): p. 188-206.

36. Garcia-Ruiz, J.M., et al., *Granada Crystallisation Box: a new device for protein crystallisation by counter-diffusion techniques*. Acta Crystallographica, Section D: Biological Crystallography, 2002. **58**(10 Part 1): p. 1638-1642.
37. Garcia- Ruiz , J.M., *The Uses of Crystal Growth in Gels and Other Diffusing-Reacting Systems*. Key Engineering Materials, 1991. **58**: p. 87-106.
38. Garcia-Ruiz, J.M., et al., *Agarose as crystallization media for proteins: I: Transport processes*. Journal of Crystal Growth, 2001. **232**(1-4): p. 165-172.
39. Bernard, Y., et al., *A gel-mediated feeding technique for protein crystal growth from hanging drops*. Acta Crystallographica, Section D: Biological Crystallography, 1994. **50**(4): p. 504-507.
40. Provost, K. and M.-C. Robert, *Application of gel growth to hanging drop technique*. Journal of Crystal Growth, 1991. **110**(1-2): p. 258-264.
41. Garcia-Ruiz, J.M. and A. Moreno, *Investigations on protein crystal growth by the gel acupuncture method*. Acta Crystallographica, Section D: Biological Crystallography, 1994. **50**(4): p. 484-490.
42. Moreno, A., D. Rondon, and J.M. Garcia-Ruiz, *Growth of shaped single crystals of proteins*. Journal of Crystal Growth, 1996. **166**(1-4): p. 919-924.
43. Ruiz, J.M.G., et al., *Crystal Quality of Lysozyme Crystals Grown by the Gel Acupuncture Method*. Materials Research Bulletin, 1991. **28**: p. 541-546.

44. J.M. Garcla-Ruiz , A.M., C. Viedma, M. Coil, *CRYSTAL QUALITY OF LYSOZYME SINGLE CRYSTALS GROWN BY THE GEL ACUPUNCTURE METHOD*. Materials Research Bulletin, 1993. **28**(541-546).
45. Nieves-Marrero, C.A., et al., *Two-step counterdiffusion protocol for the crystallization of haemoglobin II from *Lucina pectinata* in the pH range 4-9*. Acta Crystallographica, Section F: Structural Biology and Crystallization Communications, 2010. **66**(3): p. 264-268.
46. Lopez-Jaramillo, F.J., F. Otorola, and J.A. Gavira, *Protein crystal quality in diffusive environments and its evaluation*. Journal of Crystal Growth, 2003. **247**(1-2): p. 177-184.
47. Biertumpfel, C., et al., *Crystallization of biological macromolecules using agarose gel*. Acta Crystallographica, Section D: Biological Crystallography, 2002. **58**(10 Part 1): p. 1657-1659.
48. Camara-Artigas, A., et al., *Crystallization by capillary counter-diffusion and structure determination of the N114A mutant of the SH3 domain of Abl tyrosine kinase complexed with a high-affinity peptide ligand*. Acta Crystallographica, Section D: Biological Crystallography, 2007. **63**(5): p. 646-652.
49. Gavira, J.A. and J.M. Garcia-Ruiz, *Agarose as crystallisation media for proteins II: Trapping of gel fibres into the crystals*. Acta Crystallographica, Section D: Biological Crystallography, 2002. **58**(10 Part 1): p. 1653-1656.

50. Robert, M.C., Y. Bernard, and F. Lefaucheu, *Study of nucleation-related phenomena in lysozyme solutions. Application to gel growth.* Acta Crystallographica, Section D: Biological Crystallography, 1994. **50**(4): p. 496-503.
51. Vidal, O., M.C. Robert, and F. Boue, *Gel growth of lysozyme crystals studied by small angle neutron scattering: case of silica gel, a nucleation inhibitor.* Journal of Crystal Growth, 1998. **192**(1-2): p. 271-281.
52. Vidal, O., M.C. Robert, and F. Boue, *Gel growth of lysozyme crystals studied by small angle neutron scattering: case of agarose gel, a nucleation promotor.* Journal of Crystal Growth, 1998. **192**(1-2): p. 257-270.
53. Van Driessche, A.E.S., et al., *Is Agarose an Impurity or an Impurity Filter? In Situ Observation of the Joint Gel/Impurity Effect on Protein Crystal Growth Kinetics.* Crystal Growth & Design, 2008. **8**(10): p. 3623-3629.
54. Vidal, O., et al., *Crystalline quality of lysozyme crystals grown in agarose and silica gels studied by X-ray diffraction techniques.* Journal of Crystal Growth, 1999. **196**(2-4): p. 559-571.
55. Pietras, Z., et al., *The use of novel organic gels and hydrogels in protein crystallization.* Journal of Applied Crystallography, 2010. **43**(1): p. 58-63.
56. Diao, Y., et al., *Controlled Nucleation from Solution Using Polymer Microgels.* Journal of the American Chemical Society, 2011. **133**(11): p. 3756-3759.

57. Peppas, N.A., H.J. Moynihan, and L.M. Lucht, *The structure of highly crosslinked poly(2-hydroxyethyl methacrylate) hydrogels*. Journal of Biomedical Materials Research, 1985. **19**(4): p. 397-411.
58. Bell, C.L. and N.A. Peppas, *Water, solute and protein diffusion in physiologically responsive hydrogels of poly(methacrylic acid-g-ethylene glycol)*. Biomaterials, 1996. **17**(12): p. 1203-1218.
59. Garcia-Ruiz, J.M., et al., *Reinforced protein crystals*. Materials Research Bulletin, 1998. **33**(11): p. 1593-1598.
60. Maes, D., et al., *Toward a Definition of X-ray Crystal Quality* Crystal Growth & Design, 2008. **8**(12): p. 4284-4290.
61. Garcia-Ruiz, J.M., A. Moreno, C. Viedma, M. Coil, *Crystal quality of Lysozyme single crystals grown by the Gel Acupuncture Method* Materials Research Bulletin, 1993. **28**(541-546).
62. Ootaki, M., et al., *Crystal habits of cubic insulin from porcine pancreas and evaluation of intermolecular interactions by macrobond and EET analyses*. Journal of Crystal Growth, 2009. **311**(17): p. 4226-4234.
63. Gavira, J.A., et al., *Combining Counter-Diffusion and Microseeding to Increase the Success Rate in Protein Crystallization*. Crystal Growth & Design, 2011. **11**(6): p. 2122-2126.
64. Mizrahi, S., S. Eichler, and O. Ramon, *Osmotic dehydration phenomena in gel systems*. Journal of Food Engineering, 2001. **49**(2-3): p. 87-96.

APPENDICES

Appendix 1. Determination of molecular weight of monomers (\bar{M}_{n0}) by ($^1\text{H-NMR}$)

The Proton Nuclear Magnetic Resonance ($^1\text{H-NMR}$) spectra confirm the structures of the PEGDMA monomer. Spectra of PEGMA and PEGDMA are shown in figures 12 and 13 respectively. The peak positions and areas of $^1\text{H-NMR}$ spectra required to determine number average molecular weight of the polymers (\bar{M}_{n0}) are summarized in the table 7 and 8 respectively.

The spectra of PEGMA and PEGDMA show peaks at 6.13 and 5.57 ppm that correspond to vinyl protons of the end groups. The peaks at 4.29 and 3.74 ppm are methylene protons of the repeat unit. Another peak at 1.94 ppm corresponds to the methyl protons. The latter is accompanied by a peak that evidences the presence of water. The PEGMA spectrum presents one additional peak at 3.38 ppm that corresponds to the methyl protons at the chain end opposite to the methacrylate functionality.

With the peak integrals we can calculate the value of \bar{M}_{n0} of PEGMA and PEGDMA as follows:

- 1) Calculate the integral per proton from the vinyl end group signals

$$\text{Integral per proton} = \frac{\text{Sum of vinyl group integrals}}{\# \text{ of protns in the two vynil end group}}$$

- 2) Calculate the number of repeat units, n, from the methylene repeat unit signals

$$n = \frac{(\text{Sum of methylene proton integrals/ of (\# of mehhylyne protons)})}{\text{integral per proton}}$$

- 3) Calculate \bar{M}_{n0} using the formula weight of the end-groups and the repeat unit

$$\bar{M}_{n0} = (\text{FW end groups}) + (\text{FW repeat unit})(n)$$

The values calculated for PEGDMA and PEGMA were 1085.43 and 1062.85 g/mol respectively. These values are near the molecular weight reported by the manufacturer (1100 g/mol).

Table Ia. MR shifts of PEGMA

Group	δ (ppm)	Integral per proton
Water	1.887	4.6
CH3 -C(CH ₂)COO-PEG	1.943	3.05
mAcr-(CH ₂ -CH ₂ -O) _n -CH ₂ -CH ₂ -O- CH3	3.375	3
mAcr-(CH ₂ -CH ₂ -O) _n -CH ₂ - CH2 -O-CH ₃	3.544	2.05
mAcr-(CH2-CH2 -O) _n -CH ₃	3.639	81.95
CH ₃ -C(CH ₂)COO-CH ₂ - CH2 -O-PEG	3.74	2.1
CH ₃ -C(CH ₂)COO- CH2 -CH ₂ -O-PEG	4.294	2
H -CH=C(CH ₃)COO-PEG	5.571	1
H -CH=C(CH ₃)COO-PEG	6.127	1

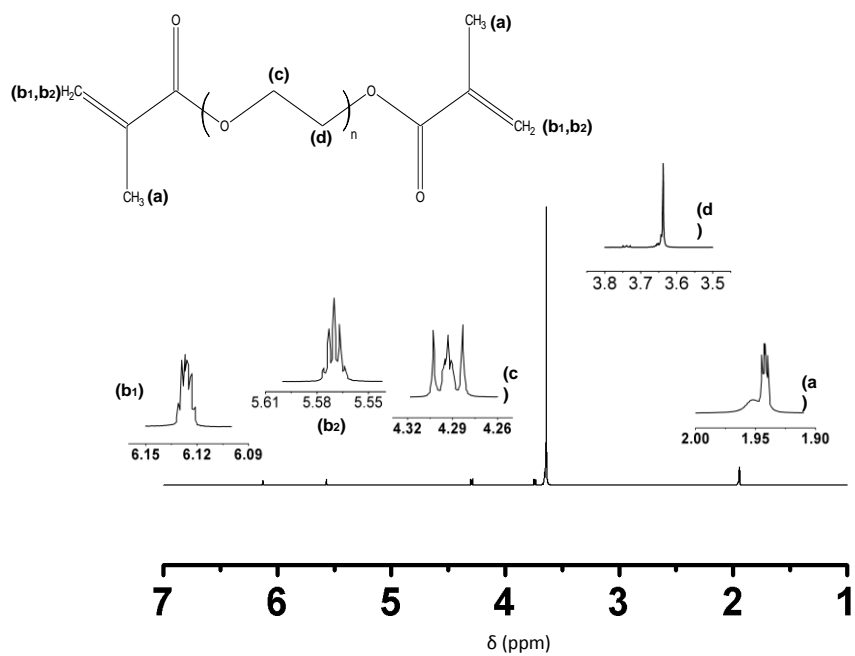


Figure Ia. The ¹H NMR spectrum of poly-ethylene glycol dimethacrylate (PEGDMA).

Table Ib. ¹H-NMR shifts of PEGDMA

Group	δ (ppm)	Integral per proton
CH3 -C(CH ₂)COO-PEG	1.942	7.4
mAcr-(CH2-CH2 -O)n-mAcr	3.638	86.8
CH ₃ -C(CH ₂)COO-CH ₂ - CH2 -O-PEG	3.739	4.8
CH ₃ -C(CH ₂)COO- CH2 -CH ₂ -O-PEG	4.293	4.2
H -CH=C(CH ₃)COO-PEG	5.57	2
H -CH=C(CH ₃)COO-PEG	6.125	2

Appendix 2. Raman spectroscopy

The Raman spectra are shown in figure 14 for solution pre-polymeric at 20 % of composition at different times. These spectra confirmed the formation of crosslinked hydrogel.

Several features became evident as a consequence of the process of polymerization that led to the formation of a crosslinked hydrogel. As depicted in figure 14 the peak at 1710 cm^{-1} presents a displacement in the crosslinked hydrogel that is attributed to an increase in the interactions between carboxylic groups and ether groups. Also, in the crosslinked hydrogel, the intensity of the band at 1630 cm^{-1} is diminished. This indicates that double bonds of the acrylate group are less abundant in the hydrogel which is expected due to the polymerization process. Also, the band at 1480 cm^{-1} changes in form, which we attribute to increased interaction between methylene groups in the network. Raman spectra provide clear evidence that the structure of the polymer has been chemically modified from the un-crosslinked monomer to the crosslinked hydrogel.

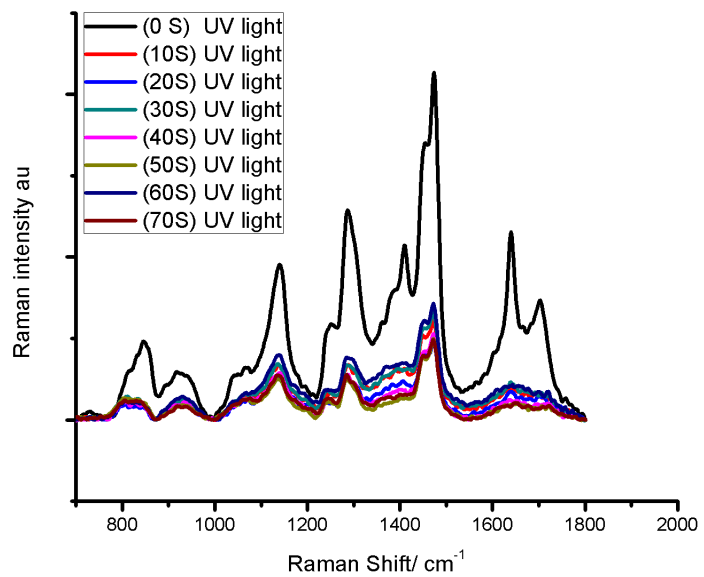


Figure IIb. Raman spectra to different times of exposition of UV light of a pre-polymeric solution (PEGDMA/PEGMA) at 20%

Appendix 3. X-ray diffraction

Finally, the identify of crystals lysozyme obtained by counterdiffusion technique in PEG hydrogel was confirmed by X-ray diffraction (see figure 11). There has been found that protein crystals diffract easily to near values 1.8 Å, showing that important information can be obtained about the structure through X- ray diffraction.

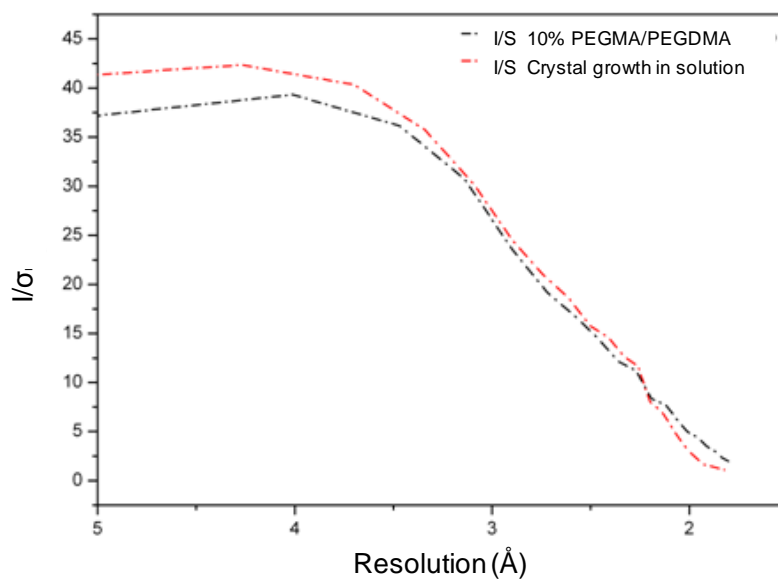


Figure IIIb. Crystallographic evaluation of the grown crystal in 10% PEG hydrogel, showing signal to noise ratio as a function of the resolution

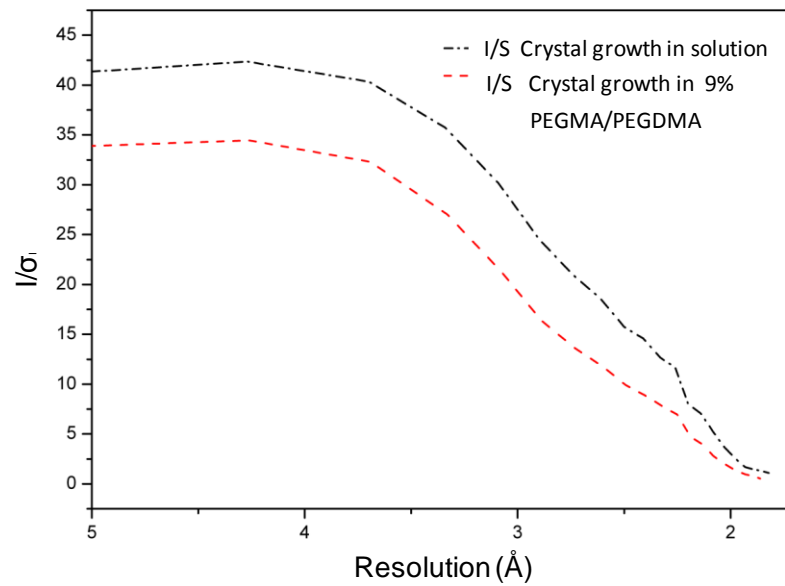


Figure IIIb. Crystallographic evaluation of the grown crystal in 9% PEG hydrogel, showing signal to noise ratio as a function of the resolution

Appendix 4 Nucleation advanced front trough the PEG hydrogel at different compositions..

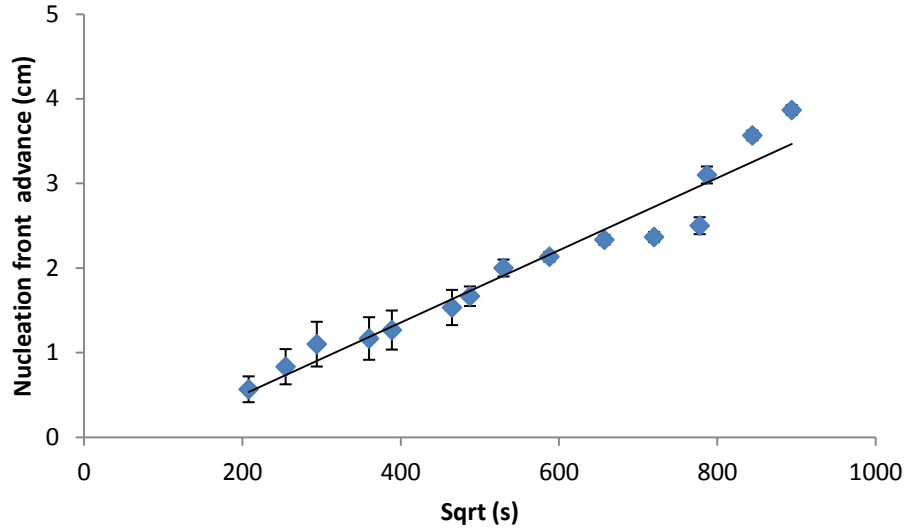


Figure Iva Nucleation advanced front through the protein chamber of 7 % PEG hydrogel prepared with 40 mg/mL protein as a solvent.

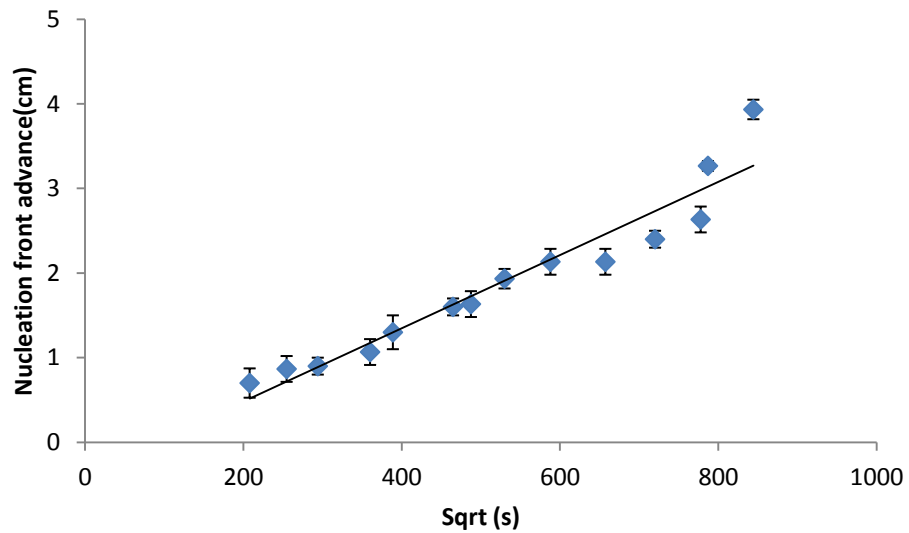


Figure Ivb Nucleation advanced front through the protein chamber of 9 % PEG hydrogel prepared with 40 mg/mL protein as a solvent.

Appendix 5. Nucleation advanced front trough the 10 % PEG hydrogel at different protein concentrations.

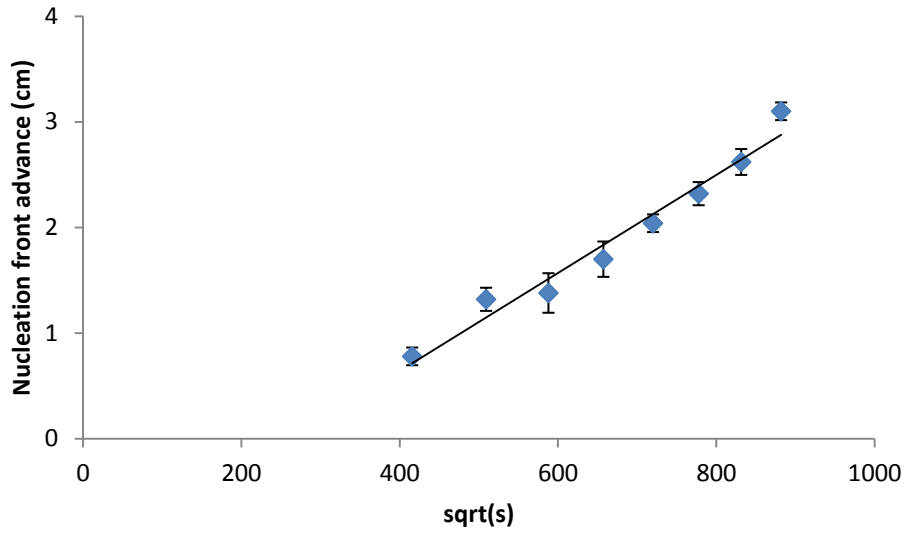


Figure Va. Nucleation advanced front through the protein chamber of 10 % PEG hydrogel prepared with 40 mg/mL protein as a solvent

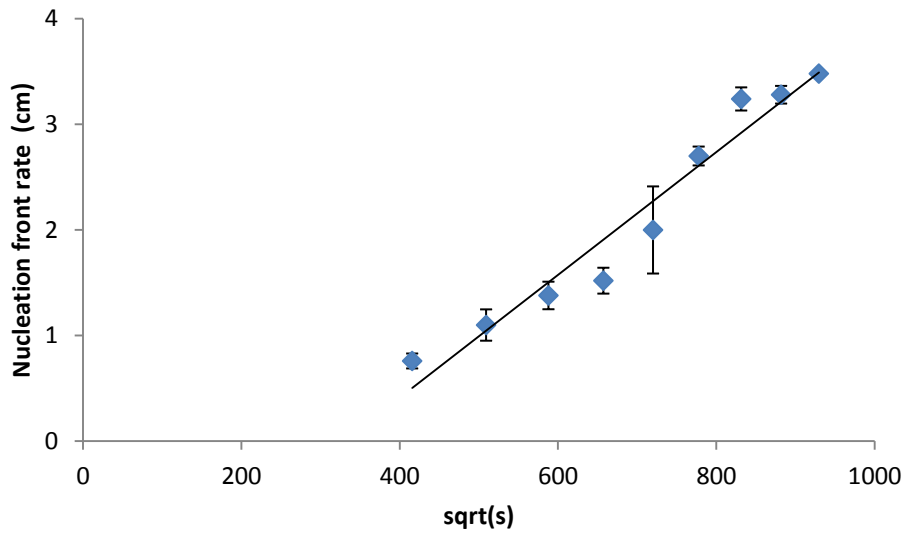


Figure IVb. Nucleation advanced front through the protein chamber of 10 % PEG hydrogel prepared with 50 mg/mL protein as a solvent

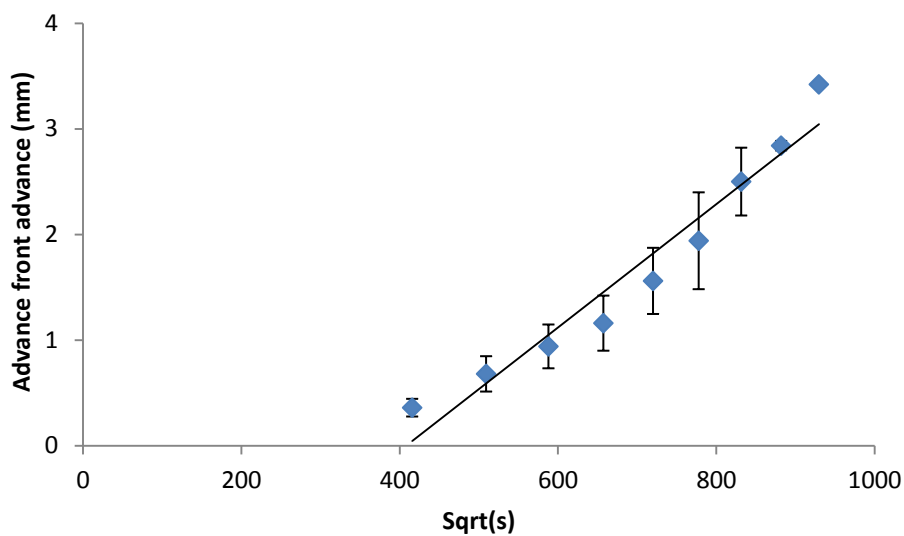


Figure Vc. Nucleation advanced front through the protein chamber of 10 % PEG hydrogel prepared with 60 mg/mL protein as a solvent

—
Appendix 6. Nucleation advanced front trough the 10 % PEG hydrogel at different PEG plug composition .

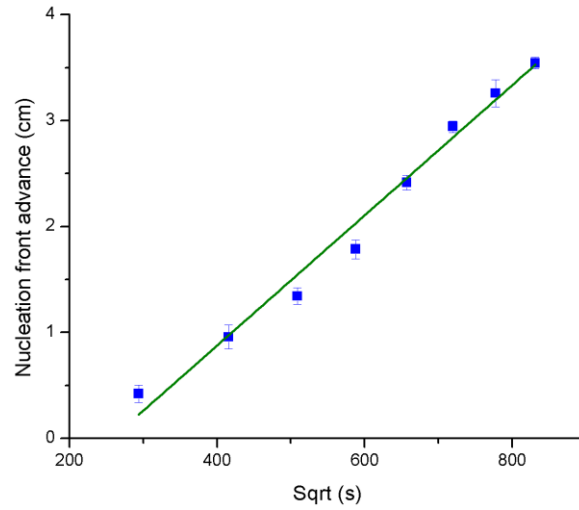


Figure VIa. Nucleation advanced front through the protein chamber of 10 % PEG hydrogel as a result of diffusion of the precipitating agent by a PEG plug composition of 20 % w/w

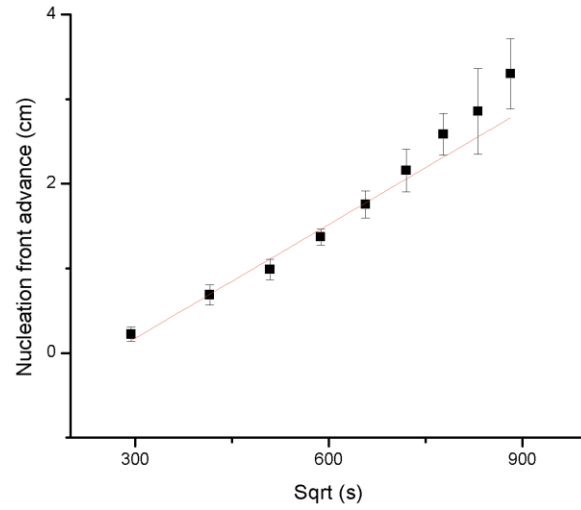


Figure VIb. Nucleation advanced front through the protein chamber of 10 % PEG hydrogel as a result of diffusion of the precipitating agent by a PEG plug composition of 35 % w/w

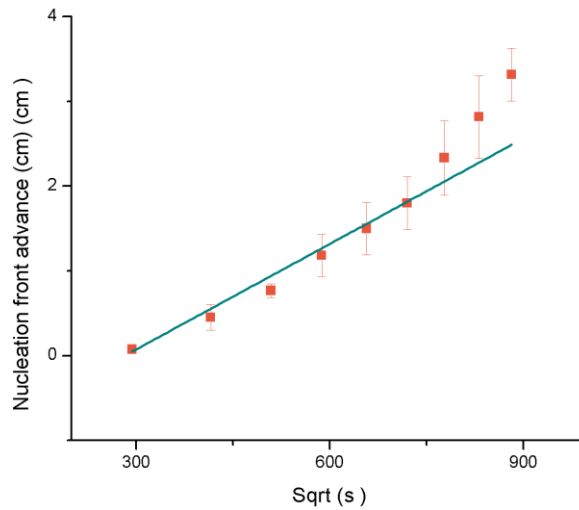


Figure VIc. Nucleation advanced front through the protein chamber of 10 % PEG hydrogel as a result of diffusion of the precipitating agent by a PEG plug composition of 50 % w/w

Appendix 7. Nucleation advanced front trough the 0.2 % w/v agarose gel at different PEG plug composition

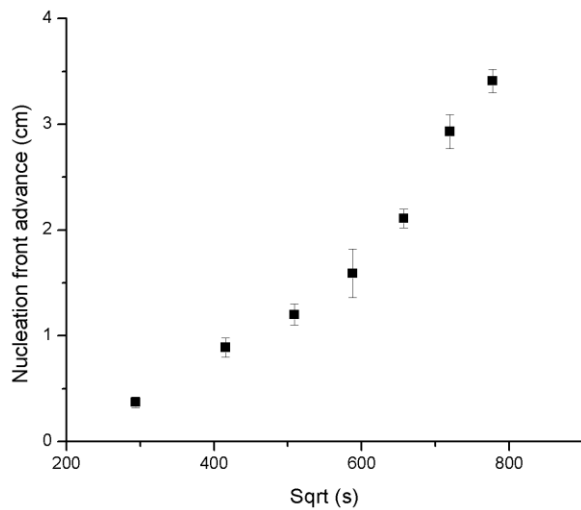


Figure VIIa. Nucleation advanced front through the protein chamber of 0.2 % w/v as a result of diffusion of the precipitating agent by a PEG plug composition of 20 % w/w

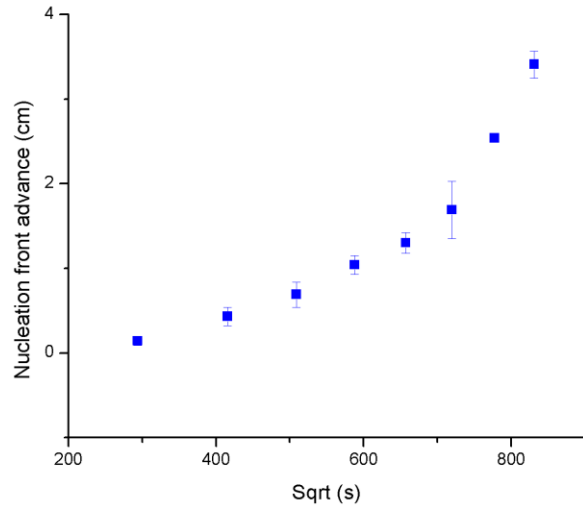


Figure VIIb. Nucleation advanced front through the protein chamber of 0.2 w/v agarose gel as a result of diffusion of the precipitating agent by a PEG plug composition of 35 % w/w

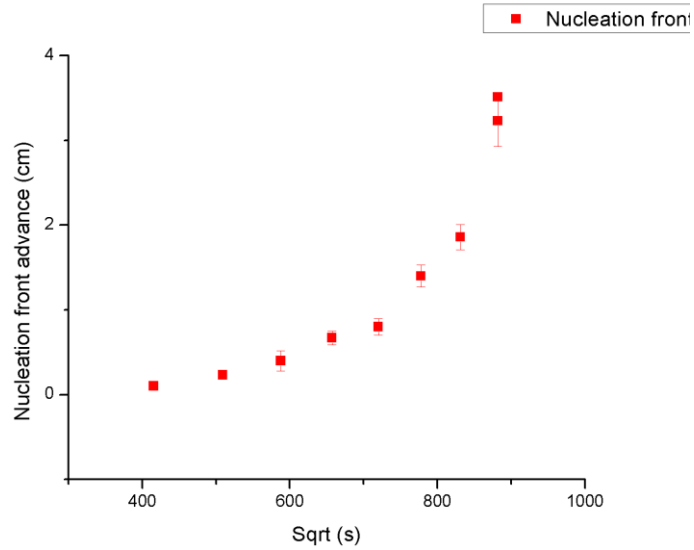


Figure VIIc. Nucleation advanced front through the protein chamber of 0.2 w/v agarose gel as a result of diffusion of the precipitating agent by a PEG plug composition of 50 % w/w